IV. The Colour Glass Condensate

A. Effective theory for the small–x gluons

- The small–x gluons $\approx$ Classical color fields radiated by the fast partons with $x' > x$

$$\Big(D_\nu F^{\nu\mu}\Big)_a(x) \;=\; J_a^\mu(x)$$

$J_a^\mu(x) =$ the color current due to the fast partons.

$D_\nu = \partial_\nu - igA_\nu^a T^a, \qquad D_\nu^{ab} = \partial_\nu \delta^{ab} - gf^{abc}A_\nu^c$

- The structure of the color current

The fast partons move nearly at the speed of light in the positive z (or x^+) direction.

$\Longrightarrow J_a^\mu$ has only a 'plus' component: $J_a^\mu = \delta^{\mu +}\rho_a$

$\Longrightarrow \rho_a$ is localized near the light-cone: $\rho_a \propto \delta(x^-)$

$\Longrightarrow \rho_a$ is independent of LC time x^+

$$\boxed{J_a^\mu(x) \;\approx\; \delta^{\mu+}\delta(x^-)\rho_a(\boldsymbol{x})}$$

- The color charge density $\rho_a(\boldsymbol{x})$: a random variable with correlations $\langle \rho \cdots \rho \rangle_x$ determined by the dynamics at the larger scales $x' > x$

$\Longrightarrow$ Weight function(al) $W_x[\rho]$ (gauge–invariant)

$$\Big\langle F_a^{+i}(x^+,\vec{x})F_a^{+i}(x^+,\vec{y})\Big\rangle_x = \int D[\rho]\; W_x[\rho]\; \mathcal{F}_a^{+i}(\vec{x})\,\mathcal{F}_a^{+i}(\vec{y})$$

$\mathcal{F}_a^{+i} = \partial^+ \mathcal{A}_a^i[\rho]$: the classical solution in LC gauge.

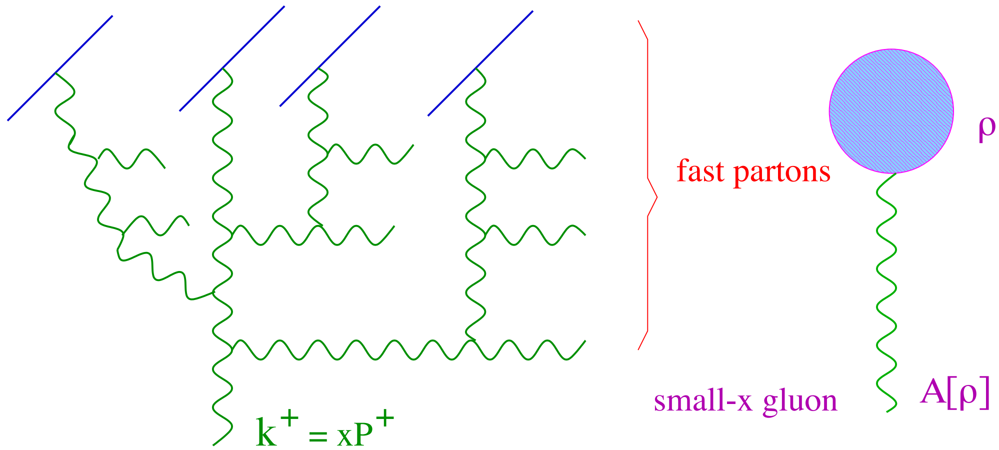

- With decreasing x, new modes become relatively fast, and must be included in the classical source ρ
  $\Longrightarrow$ Evolution of the weight function $W_x[\rho]$ with x
- Quantum evolution is computed in perturb. theory, by integrating out the fast gluons in layers of x :
  — leading–log $1/x$ for the newly radiated gluons
  — to all orders in the classical field $\mathcal{A}[\rho]$ generated by the color source constructed in previous steps
  $\Longrightarrow$ Functional evolution equation for $W_x[\rho]$:

$$\frac{\partial W_Y[\rho]}{\partial Y} = -\alpha_s \, H\left[\rho, \frac{\partial}{\partial \rho}\right] W_Y[\rho]$$

- Classical theory (a stochastic Yang–Mills theory) + Quantum evolution $\Longrightarrow$ An effective theory
- Main difference w.r.t. BFKL: non–linear effects
  $\mathcal{A} \sim 1/g$: non–linear effects must be treated exactly !
  $\longrightarrow$ exact solution $\mathcal{A}[\rho]$ to the classical EOM;
  $\longrightarrow$ exact background field quantum calculation.

Why “C G C”

- “Color” : Obvious !

- “Glass”: Separation in time scales between the small–x gluons and their fast sources

  Fast partons ($x' \gg x$) are frozen over the natural time scale for dynamics at x, namely:

  $$\tau(x) \sim \frac{2k^+}{\boldsymbol{k}^2} \sim \frac{2P^+}{\boldsymbol{k}^2}\,x$$

  One can therefore solve the dynamics of the small–x gluons at fixed distribution of the fast partons, and only then average over the latter.

  A similar situation: “spin glass”

  Collection of magnetic impurities (“spins”) randomly distributed on a non–magnetic lattice.

  spins $\longleftrightarrow$ small–x gluons

  spin <u>positions</u> $\longleftrightarrow$ color charge ρ

- “Condensate” : Coherent state with high quantum occupancy ($\sim 1/\alpha_s$ at saturation)

$$\frac{\mathrm{d}N}{\mathrm{d}Y\,\mathrm{d}^2\boldsymbol{k}\,\mathrm{d}^2\boldsymbol{b}} \sim \frac{1}{\alpha_s} \quad \text{for} \quad \boldsymbol{k}^2 \lesssim Q_s^2(Y)$$

B. The classical solution $\mathcal{A}[\rho]$

- What is the color field of a fast moving gluon ?
- Recall the corresponding problem in QED:

  The Weiszäcker–Williams field of a fast ($v \simeq c$) charged particle.
- Start in the particle rest frame: a static electric field, radially oriented (spherical symmetry).
- Make a boost with velocity v along z :

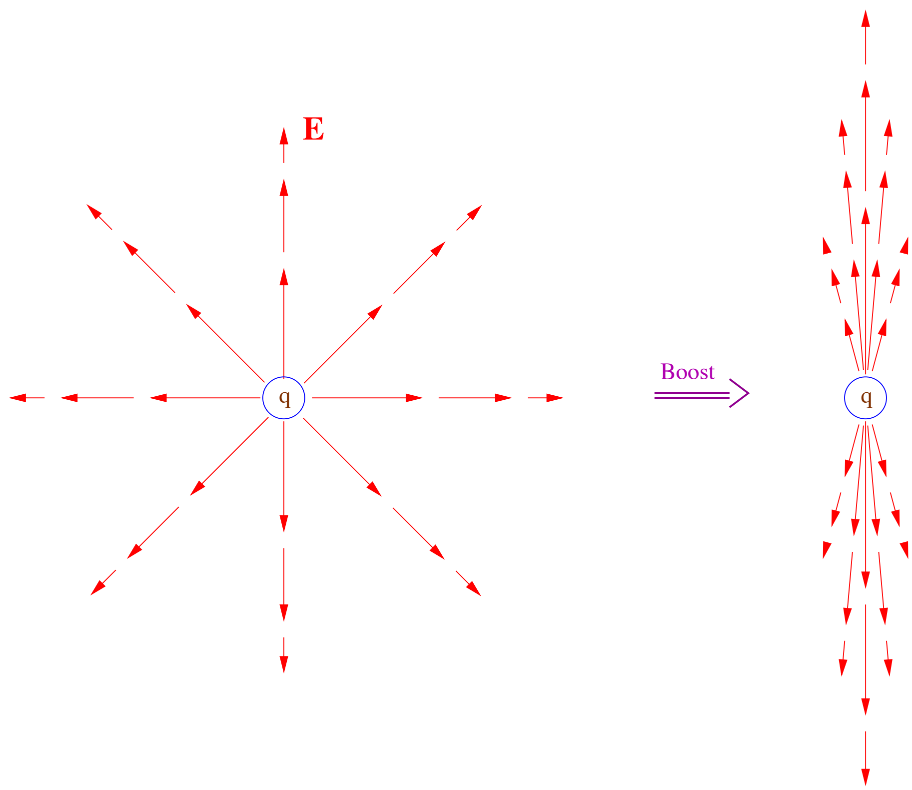

- A magnetic field is generated: $\mathbf{B} = \mathbf{v} \times \mathbf{E}$
- As $v \to c$: $E_z \to 0$ and $B_z \to 0$

  Also: $E_x = B_y\,, \quad E_y = -B_x \qquad (\mathbf{E}_\perp \cdot \mathbf{B}_\perp = 0)$

- Fields localized at $z=t$, or $x^- \equiv (t-z)/\sqrt{2} = 0$, and independent of $x^+ \equiv (t+z)/\sqrt{2}$ (plane wave)
- LC variables: the only non-zero field strength is $F^{+i} = \sqrt{2}\,E^i = \sqrt{2}\,\epsilon^{ij}B^j$
- Maxwell eqs: $\partial_\nu F^{\mu\nu} = \delta^{\mu +}\rho$ with $\rho = \delta(x^-)\rho(\boldsymbol{x})$

$$F^{+i} = \partial^i \frac{1}{\nabla_\perp^2}\,\rho \equiv -\partial^i\alpha, \qquad \text{with } -\nabla_\perp^2\alpha = \rho$$

$\alpha \equiv A^+$ in the COV–gauge $\partial^\mu A_\mu = 0$

- The non-Abelian problem: $D_\nu F^{\nu\mu} = \delta^{\mu +}\rho(\vec{x})$

The COV–gauge solution is simple again !

$$\boxed{\mathcal{A}_a^\mu(\vec{x}) = \delta^{\mu +}\alpha_a(\vec{x}) \text{ with } -\nabla_\perp^2\alpha_a = \rho_a}$$

- Explicitly

$$\alpha_a(x^-,\boldsymbol{x}) = \int \frac{\mathrm{d}^2\boldsymbol{y}}{4\pi}\,\ln\frac{1}{(\boldsymbol{x}-\boldsymbol{y})^2\Lambda^2}\,\rho_a(x^-,\boldsymbol{y})$$

$\Longrightarrow$ IR cutoff Λ^2 for the transverse dynamics

$\Longrightarrow$ locality in x^-

- But gauge–invariant observables remain non–linear, as they involve Wilson lines built with $A^+ = \alpha$!
- Obvious for dipole scattering :

$$S \Longrightarrow V^\dagger(\boldsymbol{x}) \equiv \mathrm{P}\exp\left\{ig\int \mathrm{d}x^-\alpha_a(x^-,\boldsymbol{x})t^a\right\}$$

$\boxed{\text{Exercice}}$ The gluon distribution involve the gauge-invariant operator $\mathcal{O}_\gamma$. Show that, when evaluated in the COV–gauge, this operator reads:

$$\mathcal{O}_\gamma(\vec{x},\vec{y})\Big|_{\rm COV} = \mathrm{Tr}\left\{\underbrace{V(\vec{x})\mathcal{F}^{i+}(\vec{x})V^\dagger(\vec{x})}_{\mathcal{F}^{i+}(\vec{x})|_{\rm LC}} V(\vec{y})\mathcal{F}^{i+}(\vec{y})\,V^\dagger(\vec{y})\right\}$$

$$\mathcal{F}^{i+} = \partial^i\alpha, \quad V^\dagger(x^-,\boldsymbol{x}) \equiv \mathrm{P}\,\exp\left\{ig\int_{-\infty}^{x^-}\mathrm{d}z^-\alpha_a(z^-,\boldsymbol{x})T^a\right\}$$

- NB: The longitudinal (x^-) structure of ρ (or α)

  does matter : $\mathrm{P}\,\mathrm{e}^{ig\int \mathrm{d}x^-\alpha_a(x^-)T^a} \neq \mathrm{e}^{ig\,\alpha_a T^a}$

  $\Longrightarrow$ one cannot simply use $\alpha(x^-,\boldsymbol{x}) = \delta(x^-)\alpha(\boldsymbol{x})$

  Rather: ρ (and α) is quasi–localized near $x^- = 0$

  within a distance $\Delta x^- \sim 1/k^+ = 1/xP^+$

$\boxed{\text{Smaller is } x\text{, more is the hadron (CGC) extended in } x^-}$

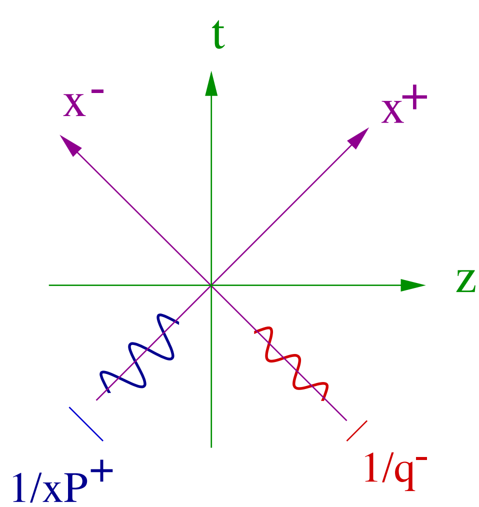

External probe: localized in x^+ ($\Delta x^+ \sim 1/q^-$) but extended in x^-: $\{A^+(x^+ \simeq 0, x^-),\ -\infty < x^- < \infty\}$

C. The gluon distribution of the valence quarks

(McLerran–Venugopalan model, 94)

- The valence quarks: the only fast partons

  — x not too small (say $x > 0.01$), so one can neglect quantum evolution;

  — a model for the initial condition for the evolution towards smaller values of x.

- Large nucleus ($A \gg 1$) [like at RHIC] :

  $\Longrightarrow$ Many color sources ($N_c \times A$) !

  $\Longrightarrow$ A strong field even without quantum evolution !

- How to formulate this as a Color Glass ?

- A small ($1/Q \ll R_p =$) dipole "sees" valence quarks from different nucleons $\Longrightarrow$ uncorrelated

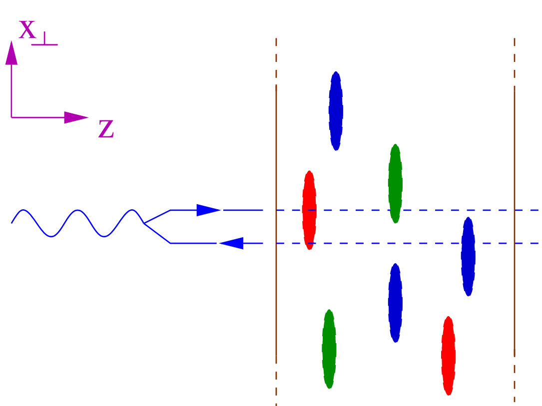

$$\langle \rho_a(\boldsymbol{x}) \rho_b(\boldsymbol{y}) \rangle_A = \delta_{ab} \delta(\boldsymbol{x} - \boldsymbol{y})\, \mu_A(\boldsymbol{x})$$

$\mu_A(\boldsymbol{x})$ = color charge squared per unit transverse area.

- Large nucleus $\approx$ homogeneous $\Longrightarrow$ no $\boldsymbol{x}$ dependence

$$\langle Q^2\rangle_A = (gt^a)(gt^a)N_c A = g^2 C_F N_c A$$

$$\langle Q^2\rangle_A = \int \mathrm{d}^2\boldsymbol{x} \int \mathrm{d}^2\boldsymbol{y}\, \langle \rho_a(\boldsymbol{x})\rho_a(\boldsymbol{y})\rangle_A = (N_c^2-1)\pi R_A^2 \mu_A$$

$$\Longrightarrow \mu_A = \frac{g^2 A}{2\pi R_A^2} = \frac{2\alpha_s A}{R_A^2} \sim \alpha_s A^{1/3}$$

- Weight function $W_A[\rho]$: a Gaussian with width μ_A
- Gluon distribution in the weak field limit

$$f_A(\boldsymbol{k}^2) = \pi \boldsymbol{k}^2 \frac{\mathrm{d}N}{\mathrm{d}Y\,\mathrm{d}^2\boldsymbol{k}} = \frac{\boldsymbol{k}^2}{(2\pi)^2} \left\langle \left| \mathcal{F}_a^{+i}(\boldsymbol{k}) \right|^2 \right\rangle_A$$

Weak fields $\Longrightarrow$ Linearized EOM $\Longrightarrow$ $\mathcal{F}^{+i} \approx i(k^i/\boldsymbol{k}^2)\rho$

$$f_A(\boldsymbol{k}^2) \approx \frac{1}{(2\pi)^2} \langle \rho_a(\boldsymbol{k})\rho_a(-\boldsymbol{k})\rangle_A$$

$$\boxed{f_A(\boldsymbol{k}^2) \approx A N_c\,(\alpha_s C_F/\pi) \equiv A N_c\, f_q(\boldsymbol{k}^2)}$$

- The integrated gluon distribution (weak field)

$$xG_A(x,Q^2) \approx (N_c^2-1)\pi R_A^2 \int^{Q^2} \frac{\mathrm{d}\boldsymbol{k}^2}{(2\pi)^2} \frac{\mu_A}{\boldsymbol{k}^2}$$

$$\approx A N_c \frac{\alpha_s C_F}{\pi} \ln \frac{Q^2}{\Lambda^2}$$

$\Longrightarrow$ Infrared divergence !

Why ? No $x_\perp$–correlations among the color sources !

- One expects quantum evolution towards small x to introduce correlations and energy dependence :

$$\boxed{\mu_A \longrightarrow \mu_A(Y,\boldsymbol{k})}$$

D. The Renormalization Group at Small–x

- ρ and its correlators change with decreasing x.
- Because of non–linear effects, the evolution couples n–point functions $\langle \rho(1)\rho(2)\cdots\rho(n)\rangle_x$ with different n.
- It is most conveniently formulated as a functional evolution equation for the weight function $W_x[\rho]$
- Strategy: Integrate out quantum fluctuations in layers of k^+ (or of x, or of rapidity $Y = \ln(1/x)$).

  i) Start with the effective theory at scale $\Lambda^+ = xP^+$. The fast partons with $k^+ > \Lambda^+$ have been already integrated out.

  ii) Compute correlation functions at a new scale $b\Lambda^+$ with $b \ll 1$ but such that $\alpha_s \ln(1/b) < 1$.

  These include:

  — classical correlations associated with ρ and described by $W_x[\rho]$

  — quantum correlations associated with the 'semi–fast' partons with $b\Lambda^+ < k^+ < \Lambda^+$.

  Quantum corrections are computed to $O(\alpha_s \ln(1/b))$ but to all orders in the classical field $\mathcal{A}[\rho]$

  iii) Reinterpret the quantum corrections as classical correlations associated with a (functional) change in the weight function: $W_x[\rho] \to W_{x'}[\rho] = W_x + \mathrm{d}W_x$ (with $x' = bx \ll x$). This fixes $\mathrm{d}W_x[\rho]$.

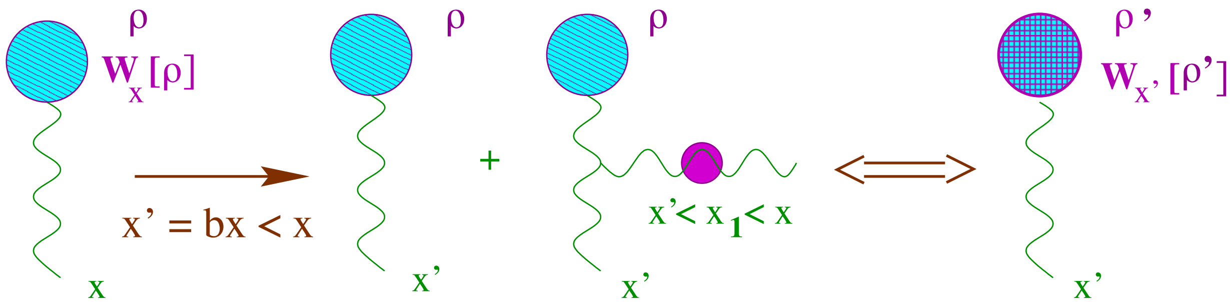

- One-loop calculation with the Background–Field Propagator:

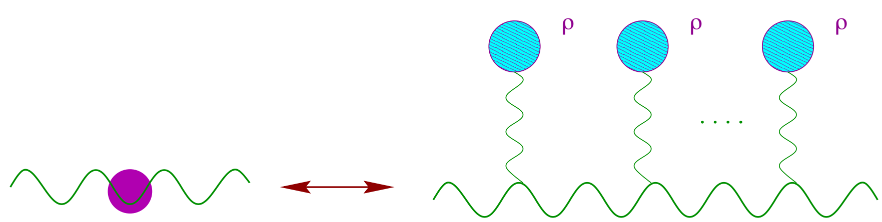

- Since $\mathrm{d}W_x \propto \alpha_s \ln(x/x') \equiv \alpha_s \mathrm{d}Y$, this evolution is rewritten as a differential equation in Y :

$$\frac{\partial W_Y[\rho]}{\partial Y} = \frac{1}{2}\int_{\boldsymbol{x},\boldsymbol{y}} \frac{\delta}{\delta\rho_Y^a(\boldsymbol{x})}\, \chi_{\boldsymbol{xy}}^{ab}[\rho]\, \frac{\delta}{\delta\rho_Y^b(\boldsymbol{y})}\, W_Y[\rho]$$

Renormalization Group Equation at small–x.

Also known as "JIMWLK equation" (cf. A. Mueller)

Jalilian-Marian, Kovner, Leonidov, Weigert, 97; Weigert, 2000; Iancu, Leonidov, McLerran, 2000

- A <u>second–order</u> functional differential equation.

- At each step $Y \to Y + \mathrm{d}Y$ in the evolution, only the 1-point and 2-point correlations of ρ need be adjusted:

$$\chi^{ab}(\boldsymbol{x},\boldsymbol{y})[\rho] = \langle \delta\rho^a_Y(\boldsymbol{x})\delta\rho^b_Y(\boldsymbol{y})\rangle_\rho, \quad \sigma^a(\boldsymbol{x})[\rho] = \langle \delta\rho^a_Y(\boldsymbol{x})\rangle_\rho$$

- χ, σ : generalizations of the real and virtual parts of the BFKL kernel including background field effects :

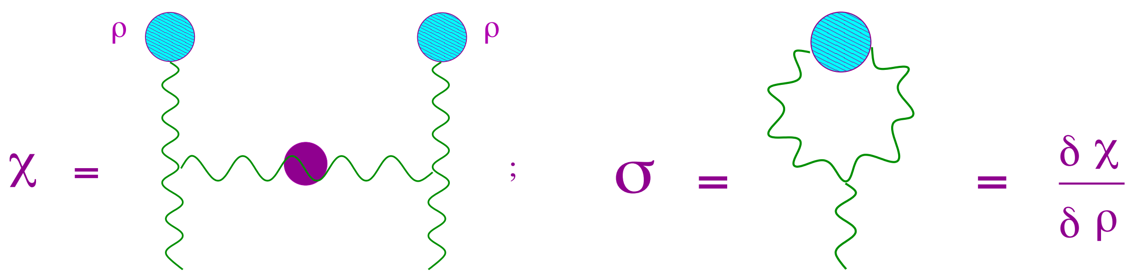

$$\sigma^a(\boldsymbol{x}) = \frac{1}{2}\int \mathrm{d}^2\boldsymbol{y}\, \frac{\delta\chi^{ab}(\boldsymbol{x},\boldsymbol{y})}{\delta\rho^b_Y(\boldsymbol{y})}$$

Functional relation $\sigma \longleftrightarrow \chi$ ensures the cancellation of infrared divergences in gauge–invariant quantities.

- Change of variables : $\rho_a \longrightarrow \alpha_a$ with $-\nabla^2_\perp \alpha_a = \rho_a$

$$\frac{\partial W_Y[\alpha]}{\partial Y} = \frac{1}{2}\int_{\boldsymbol{x},\boldsymbol{y}} \frac{\delta}{\delta\alpha^a_Y(\boldsymbol{x})}\, \chi^{ab}_{\boldsymbol{xy}}[\alpha]\, \frac{\delta}{\delta\alpha^b_Y(\boldsymbol{y})}\, W_Y[\alpha]$$

- χ depends upon α via Wilson lines:

$$\chi^{ab}_{\boldsymbol{xy}}[\alpha] \equiv \int \frac{\mathrm{d}^2\boldsymbol{z}}{\pi}\, \mathcal{K}_{\boldsymbol{xyz}} \Big[(1 - V^\dagger_{\boldsymbol{x}} V_{\boldsymbol{z}})(1 - V^\dagger_{\boldsymbol{z}} V_{\boldsymbol{y}})\Big]^{ab}$$

$$\mathcal{K}_{\boldsymbol{xyz}} \equiv \frac{1}{(2\pi)^2}\frac{(\boldsymbol{x}-\boldsymbol{z})\cdot(\boldsymbol{y}-\boldsymbol{z})}{(\boldsymbol{x}-\boldsymbol{z})^2(\boldsymbol{z}-\boldsymbol{y})^2}$$

- The coupling g enters only via the Wilson lines !

E. General consequences of the RGE

1. Longitudinal (x^-) structure of α (or ρ)

- RGE: non–local in $x_\perp$ and in x^-

$$V^\dagger(\boldsymbol{x}) \equiv \mathrm{P}\,\exp\left\{ ig \int \mathrm{d}x^- \alpha_a(x^-, \boldsymbol{x}) T^a \right\}$$

- With decreasing x, the classical field extends in x^-

Lower $k^+ = xP^+ \quad \Longleftrightarrow \quad$ Increase $\Delta x^- \sim 1/k^+$

- For the theory at scale Λ^+, the support of the field is retricted to: $x^- < 1/\Lambda^+$

$\Lambda^+ \to b\Lambda^+ \Longrightarrow \delta\alpha_\Lambda$ with support at $1/\Lambda^+ < x^- < 1/b\Lambda^+$

The new field $\delta\alpha_\Lambda$ has no overlap with the previous one.

- The CGC is built in layers of x^-.

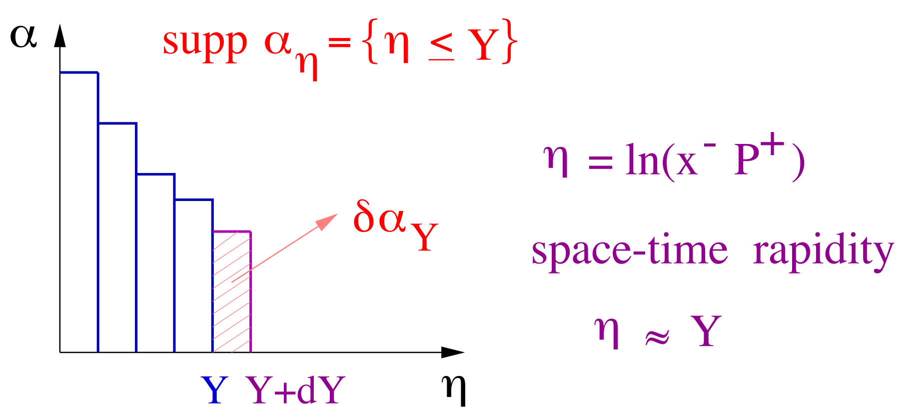

- Wilson lines evolve by left (or right) multiplication:

$$V^\dagger_{Y+\mathrm{d}Y} = \mathrm{e}^{ig\,\delta\alpha^a_Y T^a}\, V^\dagger_Y$$

$$\frac{\delta}{\delta\alpha^a_Y(\boldsymbol{x})} V^\dagger_Y(\boldsymbol{y}) = igT^a V^\dagger_Y(\boldsymbol{x})\delta(\boldsymbol{x}-\boldsymbol{y})$$

2. Quantum Evolution as a Random Walk

- Since $\delta\alpha_Y \equiv \alpha_Y \mathrm{d}Y$ is a random quantity, the evolution defines a random walk on SU(3) :

$$Y = n\epsilon, \qquad V_n^\dagger(\boldsymbol{x}) = \mathrm{e}^{\,\mathrm{i}\epsilon\alpha_n^a(\boldsymbol{x})T^a}\, V_{n-1}^\dagger(\boldsymbol{x})$$

$$\langle \alpha_n^a(\boldsymbol{x})\rangle = \sigma_{n-1}^a(\boldsymbol{x}), \quad \langle \alpha_n^a(\boldsymbol{x})\alpha_n^b(\boldsymbol{y})\rangle = \frac{1}{\epsilon}\,\chi_{n-1}^{ab}(\boldsymbol{x},\boldsymbol{y})$$

σ_{n-1} and χ_{n-1} : functionals of V_{n-1}

- RGE: A functional Fokker–Planck equation with "time" Y and "diffusion coefficient" $\chi[\rho] \geq 0$.

  Blaizot, E.I., Weigert, 2002

- Recent numerical solution (lattice)

  Rummukainen, Weigert, sept. 2003

- Recall: <u>Brownian motion</u>

Small particle in a viscous liquid $\Longrightarrow$ Random velocity:

$$\mathrm{d}x^\alpha/\mathrm{d}t = v^\alpha(t), \qquad \langle v^\alpha(t)v^\beta(t')\rangle = \nu\,\delta^{\alpha\beta}\delta(t-t')$$

with $\alpha, \beta = \overline{1,3}$. With discretized time: $t = n\epsilon$

$$x_n^\alpha - x_{n-1}^\alpha = \epsilon\, v_n^\alpha, \qquad \langle v_n^\alpha\, v_r^\beta\rangle = (1/\epsilon)\,\nu\,\delta^{\alpha\beta}\,\delta_{nr}$$

- $P(\boldsymbol{x}, t)$: probability to find the particle at point $\boldsymbol{x}$ at time t. This obeys the diffusion (or FP) equation:

$$\frac{\partial P(\boldsymbol{x},t)}{\partial t} = D\,\frac{\partial^2 P(\boldsymbol{x},t)}{\partial x^\alpha \partial x^\alpha}\,, \qquad D \equiv \nu^2$$

- $\langle(\boldsymbol{x}-\boldsymbol{x}_0)^2\rangle(t) = 6Dt$: "runaway solution"

3. Evolution equations for correlations

- A functional, non–linear, equation for $W_Y[\alpha]$

  $\Longleftrightarrow$ An infinite hierarchy of ordinary equations for the n–point functions $\langle \alpha(1)\alpha(2)\cdots\alpha(n)\rangle_Y$

- $O[\alpha]$: any observable or correlation functions :

$$\langle O[\alpha]\,\rangle_Y \,=\, \int D[\alpha]\, O[\alpha]\, W_Y[\alpha]$$

  Take a derivative w.r.t. Y and use the RGE:

$$\frac{\partial}{\partial Y}\,\langle O[\alpha]\rangle_Y \;=\; \int D[\alpha]\, O[\alpha]\, \frac{\partial W_Y[\alpha]}{\partial Y}$$

$$=\; \left\langle \frac{1}{2}\int_{\boldsymbol{xy}} \frac{\delta}{\delta\alpha_Y^a(\boldsymbol{x})}\,\chi^{ab}_{\boldsymbol{xy}}\,\frac{\delta}{\delta\alpha_Y^b(\boldsymbol{y})}\, O[\alpha]\right\rangle_Y$$

- Example: $O[\alpha] = \langle \alpha(\boldsymbol{x})\alpha(\boldsymbol{y})\rangle_Y$

$$\frac{\partial}{\partial Y}\langle \alpha(\boldsymbol{x})\alpha(\boldsymbol{y})\rangle_Y = \langle \chi(\boldsymbol{x},\boldsymbol{y})\rangle_Y + \langle \sigma(\boldsymbol{x})\alpha(\boldsymbol{y})\rangle_Y + \langle \alpha(\boldsymbol{x})\sigma(\boldsymbol{y})\rangle_Y$$

  Via the Wilson lines within χ and σ, the r.h.s. involves all the n–point functions with $n \geq 2$!

- Weak field (low density) regime: $g\alpha \ll 1$

  $V^\dagger(\boldsymbol{x}) \approx 1 + ig\int \mathrm{d}x^-\alpha(x^-,\boldsymbol{x}) \equiv 1 + ig\alpha(\boldsymbol{x})$

  $1 - V^\dagger_{\boldsymbol{x}} V_{\boldsymbol{z}} \approx -ig\big(\alpha(\boldsymbol{x}) - \alpha(\boldsymbol{z})\big)$

  $\Longrightarrow$ χ is quadratic in α, and σ is linear:

$$\chi \sim g^2\alpha^2, \quad \sigma \sim g^2\alpha$$

  $\Longrightarrow$ Closed equation for the 2-point function: BFKL

- Strong field (high density) regime: $g\alpha \sim 1$

  This is relevant for correlations over large transverse separations, or soft momenta:

  $|\boldsymbol{x}-\boldsymbol{y}| \gtrsim 1/Q_s(Y)$ or $\boldsymbol{k}^2 \lesssim Q_s^2(Y)$

  $g\alpha(\boldsymbol{x}) \sim 1$ and strongly varying over a (relatively short) distance $\Delta x_\perp \sim 1/Q_s(Y)$

  $\Longrightarrow$ Wilson lines V, $V^\dagger$: complex exponentials which oscillate around zero over a distance $\sim 1/Q_s(Y)$

- When probed over distances large compared to $1/Q_s$, the Wilson lines average to zero: $V,\, V^\dagger \approx 0$

$$\boxed{\langle V^\dagger(\boldsymbol{x})V(\boldsymbol{y})\rangle_Y \ll 1 \text{ for } |\boldsymbol{x}-\boldsymbol{y}| \gg 1/Q_s(Y)}$$

$\boxed{\text{Exercice}}$ Show than, when $V,\, V^\dagger \approx 0$:

$$\chi^{ab}(\boldsymbol{x},\boldsymbol{y}) \approx \delta^{ab}\frac{1}{\pi}\langle \boldsymbol{x}|\frac{1}{-\nabla_\perp^2}|\boldsymbol{y}\rangle, \quad \chi^{ab}(\boldsymbol{k}) \approx \delta^{ab}\frac{1}{\pi \boldsymbol{k}^2}$$

- The RGE reduces to free Brownian motion (no g !) $\Longrightarrow$ Duality at Saturation [E.I., McLerran 01]

- In particular, the evolution of the 2-point function reduces to :

$$\frac{\partial}{\partial Y}\langle \alpha(\boldsymbol{k})\alpha(-\boldsymbol{k})\rangle_Y \approx \frac{1}{\pi \boldsymbol{k}^2}$$

F. Non–Linear Gluon Evolution: Saturation & Geometric Scaling

- Focus on the charge–charge correlator $\langle \rho(\boldsymbol{x})\rho(\boldsymbol{y})\rangle_Y$:

  i) Interesting information about the spatial distribution of the color charges.

  ii) Access to the gluon distribution:

$$f(Y,\boldsymbol{k}^2) \propto \langle \rho_a(\boldsymbol{k})\rho_a(-\boldsymbol{k})\rangle_Y$$

- Initial condition: $x \simeq 10^{-1}\cdots 10^{-2} \Longrightarrow$ MV model

$$\boxed{\langle \rho_a(\boldsymbol{k})\rho_a(-\boldsymbol{k})\rangle_Y \;=\; \mu_0 \qquad \text{(no correlation)}}$$

- Weak fields $(\boldsymbol{k}^2 \gg Q_s^2(Y)) \Longrightarrow$ BFKL

$$\boxed{\langle \rho_a(\boldsymbol{k})\rho_a(-\boldsymbol{k})\rangle_Y \;\approx\; \sqrt{\mu_0\,\boldsymbol{k}^2}\,\mathrm{e}^{\omega\alpha_s Y}}$$

- Strong fields $(\boldsymbol{k}^2 \ll Q_s^2(Y)) \Longrightarrow$ Free diffusion

$$\boxed{\langle \rho_a(\boldsymbol{k})\rho_a(-\boldsymbol{k})\rangle_Y \;\approx\; (\boldsymbol{k}^2/\pi)\,\big(Y - Y_s(\boldsymbol{k})\big)}$$

- $Y - Y_s(\boldsymbol{k})$ = rapidity excursion in the saturation regime for a given $\boldsymbol{k}$:

$$Q_s^2(Y) = \boldsymbol{k}^2 \quad \text{for} \quad Y = Y_s(\boldsymbol{k})$$

$$Q_s^2(Y) = Q_0^2\,\mathrm{e}^{\,c\alpha_s Y} \Longrightarrow Y - Y_s(\boldsymbol{k}) = \frac{1}{c\alpha_s}\ln\frac{Q_s^2(Y)}{\boldsymbol{k}^2}$$

1. Color Neutrality at Saturation

$$\langle \rho(\boldsymbol{k})\rho(-\boldsymbol{k})\rangle_Y \;\propto\; \boldsymbol{k}^2 \quad \text{for} \quad \boldsymbol{k}^2 < Q_s^2(Y)$$

$\Longrightarrow$ Improved infrared behaviour

The behaviour expected from gauge symmetry !

Recall: In QED, the charge–charge correlator $\Pi_{00}(k) = \langle\rho\rho\rangle$ vanishes like k^2 as $k \to 0$.

- Physical interpretation:

  Color neutrality over a typical size $1/Q_s(\tau)$

$$Q^a|_{\Delta\Sigma} \equiv \int_{\Delta\Sigma} \mathrm{d}^2\boldsymbol{x}\;\rho_a(\boldsymbol{x}) \;\simeq\; 0 \quad \text{for} \quad \Delta\Sigma \gtrsim 1/Q_s^2$$

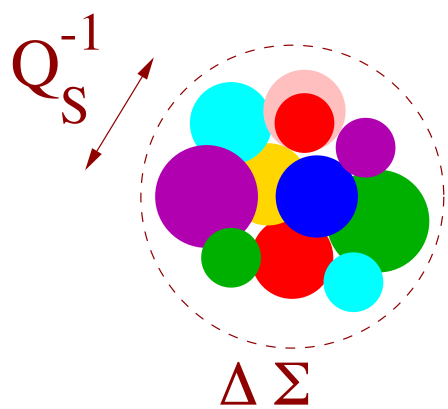

- The densely packed gluons shield their color charges each other, to diminish their mutual repulsion, and thus allow for a maximal density state.

  (E.I., McLerran 01; A. Mueller, 02)

- When "seen" over distance scales $\Delta x_\perp > 1/Q_s(Y)$, the gluons generate only dipolar color fields !

2. Gluon Saturation

- Gluon occupation number :

$$n_g \equiv \frac{(2\pi)^3}{2\cdot(N_c^2-1)}\,\frac{\mathrm{d}N}{\mathrm{d}Y\,\mathrm{d}^2\boldsymbol{k}\,\mathrm{d}^2\boldsymbol{b}} \simeq \frac{\langle\rho_a(\boldsymbol{k})\rho_a(-\boldsymbol{k})\rangle_Y}{\boldsymbol{k}^2}$$

- Very large $\boldsymbol{k}$: $\ln\boldsymbol{k}^2 \gg \alpha_s Y$ (MV model, DGLAP) :

$$n_g(Y,\boldsymbol{k}) \approx \frac{\mu_0}{\boldsymbol{k}^2}$$

- $\ln\boldsymbol{k}^2 \sim \alpha_s Y$ but $\boldsymbol{k}^2 \gg Q_s^2(Y)$ (BFKL) :

$$n_g(Y,\boldsymbol{k}) \approx \left(\frac{\mu_0}{\boldsymbol{k}^2}\right)^{1/2} \mathrm{e}^{\omega\alpha_s Y} \propto \frac{1}{x^{\omega\alpha_s}}$$

- $\boldsymbol{k}^2 \ll Q_s^2(Y)$: $\quad n_g(Y,\boldsymbol{k}) \approx \frac{1}{\alpha_s}\ln\frac{Q_s^2(Y)}{\boldsymbol{k}^2} \propto \ln\frac{1}{x}$

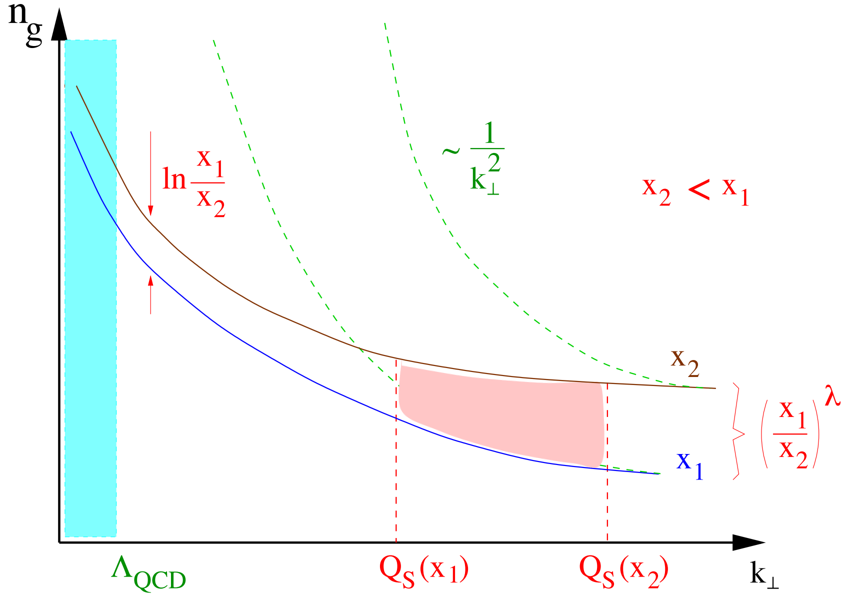

- Power–law increase with $1/\boldsymbol{k}$ and $1/x$ is replaced by logarithmic behaviour $\Longrightarrow$ (marginal) saturation

- Condensate at Saturation:

$$n_g(k_\perp \lesssim Q_s(Y)) \sim 1/\alpha_s$$

- With increasing Y, new gluons are produced predominantly at high momenta $\gtrsim Q_s(Y)$.

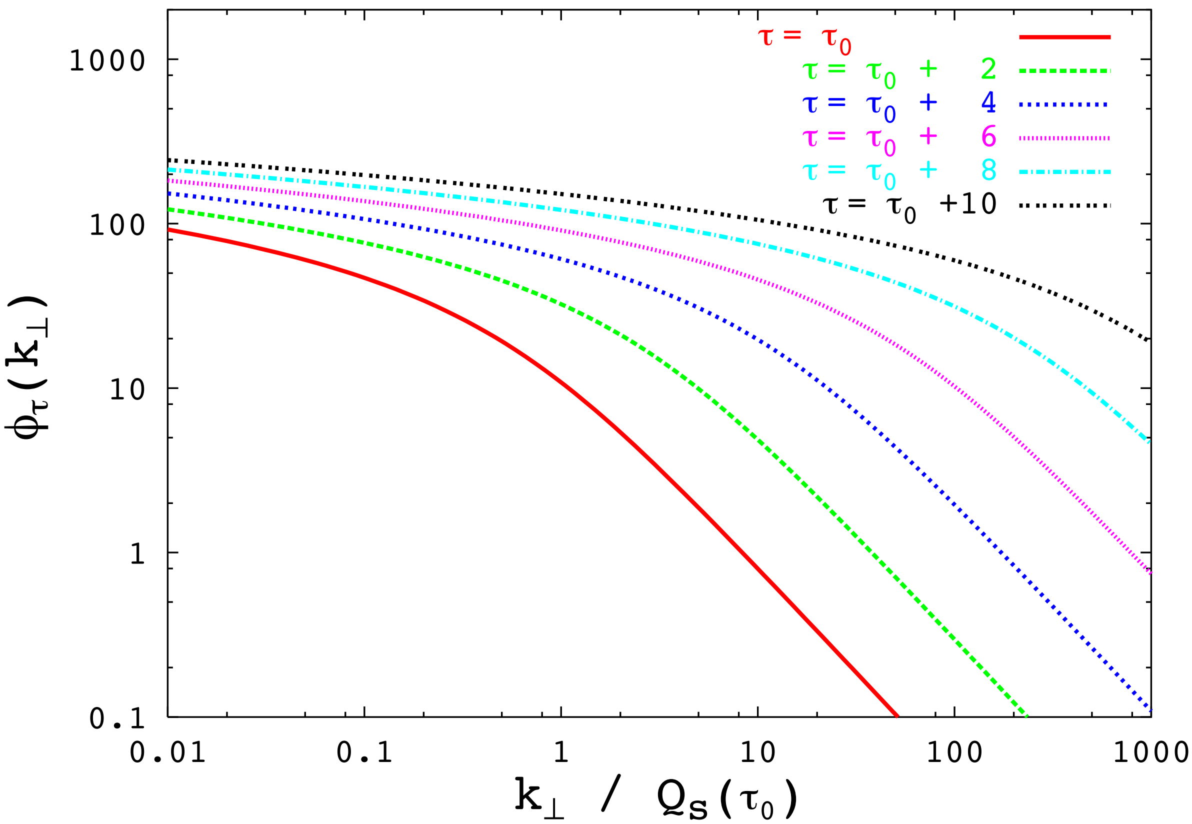

NB: Different notations:

$\tau \equiv Y$ and $\phi_\tau(k_\perp) \equiv n_g(Y, k_\perp)$

- What is the saturation momentum ?

3. Saturation Momentum

- How to compute $Q_s(Y)$?
- Approach the saturation scale from the above ($k_\perp \gg Q_s(Y)$), where the linear BFKL eq. applies, and use the saturation condition at $k_\perp \simeq Q_s(Y)$.
- Saturation condition :

$$n_g(Y,\boldsymbol{k}) \sim \frac{1}{\alpha_s} \quad \text{for} \quad k \sim Q_s(Y)$$

- BFKL solution ($k_\perp \gg Q_s(Y)$) :

$$n_g(Y,\boldsymbol{k}) \approx \left(\frac{Q_0^2}{\boldsymbol{k}^2}\right)^{1/2} \mathrm{e}^{\omega\bar{\alpha}_s Y} \exp\left\{-\frac{\ln^2\left(\boldsymbol{k}^2/Q_0^2\right)}{2\beta\bar{\alpha}_s Y}\right\}$$

Exercice: Show that the saturation condition together with the BFKL solution imply:

$$Q_s^2(Y) = Q_0^2\,\mathrm{e}^{\,c\bar{\alpha}_s Y}\,, \qquad c \equiv \frac{-\beta + \sqrt{\beta(\beta+8\omega)}}{2} = 4.84...$$

- Controlled up to terms $O(\ln Y)$ in the exponent.
- Replace $Q_0^2 \to Q_s^2(Y)$ as the reference scale :

$$\ln\frac{\boldsymbol{k}^2}{Q_0^2} = \ln\frac{\boldsymbol{k}^2}{Q_s^2(Y)} + c\bar{\alpha}_s Y$$

$$n_g(Y,\boldsymbol{k}) \approx \frac{1}{\alpha_s}\left(\frac{Q_s^2(Y)}{\boldsymbol{k}^2}\right)^{\gamma_s} \exp\left\{-\frac{\ln^2\left(\boldsymbol{k}^2/Q_s^2(Y)\right)}{2\beta\bar{\alpha}_s Y}\right\}$$

where $\gamma_s \equiv 1/2 + c/\beta \approx 0.64$.

4. Geometric Scaling

- The previous results suggests that for $k_\perp \leq Q_s(Y)$:

$$n_g(Y, \boldsymbol{k}) \approx \frac{A}{\bar{\alpha}_s} \left(\ln \frac{Q_s^2(Y)}{\boldsymbol{k}^2} + B \right)$$

where the numbers A and B are not under control.

- At saturation, the gluon distribution:

i) scales as a function of $\tau \equiv Q_s^2(Y)/\boldsymbol{k}^2$;

ii) it is marginally universal : it depends upon the initial conditions only logarithmically, via Q_s.

- What about $k_\perp$ above but near Q_s ?

$$n_g(Y, \boldsymbol{k}) \approx \frac{C}{\bar{\alpha}_s} \left(\frac{Q_s^2(Y)}{\boldsymbol{k}^2} \right)^{\gamma_s} \exp \left\{ -\frac{\ln^2 \left(\boldsymbol{k}^2 / Q_s^2(Y) \right)}{2\beta \bar{\alpha}_s Y} \right\}$$

- If $k > Q_s$, but $\ln \left(\boldsymbol{k}^2 / Q_s^2(Y) \right) \ll \bar{\alpha}_s Y$, the diffusion term can be neglected:

$$n_g(Y, \boldsymbol{k}) \approx \frac{C}{\bar{\alpha}_s} \left(\frac{Q_s^2(Y)}{\boldsymbol{k}^2} \right)^{\gamma_s}$$

$\Longrightarrow$ approximate scaling persists above Q_s !

$$\boxed{\text{New anomalous dimension: } \gamma_s \approx 0.64}$$

- A natural explanation for the “geometric scaling” recently identified in the HERA data (see below).

[Staśto, Golec-Biernat, and Kwieciński, 2000]

A "phase-diagram" for high-energy QCD

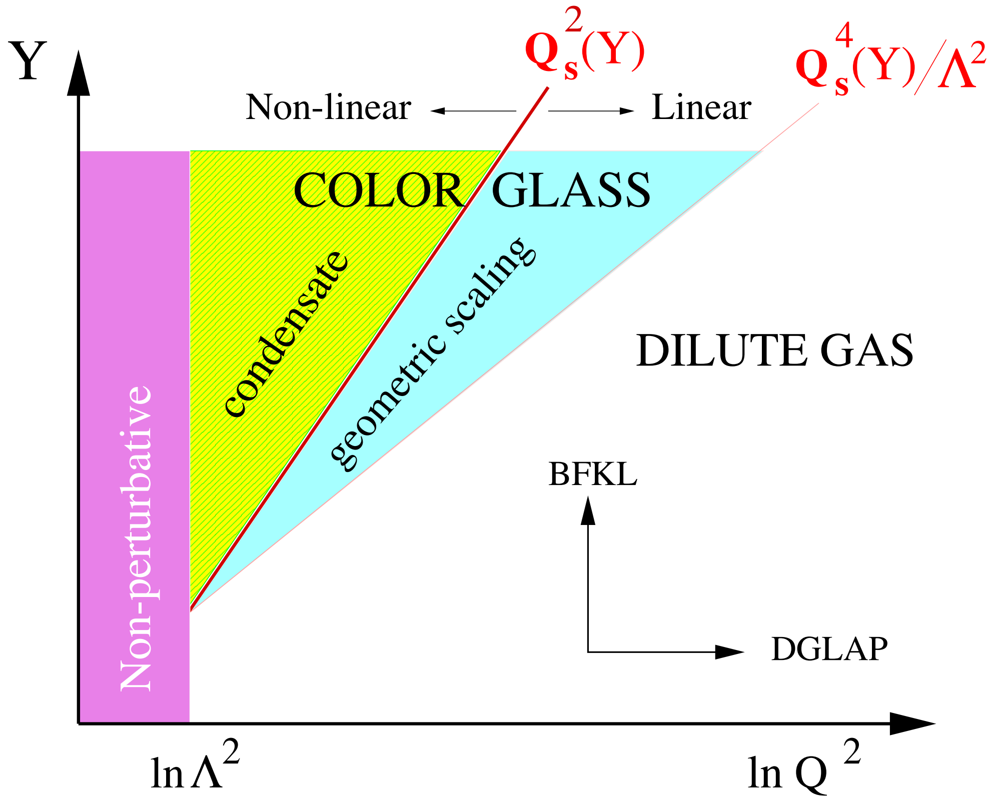

- Saturation line: $Q_s^2(Y) \simeq Q_0^2\, \mathrm{e}^{\lambda Y}$

  $\lambda = 4.84(\alpha_s N_c/\pi) \simeq 1$ at LO BFKL level

  $\lambda \approx 0.3$ for $Y = 5 \cdots 9$ from NLO BFKL equation

  (Triantafyllopoulos, 02)

- "Extended scaling" : $Q_s^2(Y) < Q^2 < Q_s^4(Y)/Q_0^2$

  Scaling window $\approx$ BFKL window

- Scaling violation by the "diffusion" term

V. DIS off the C G C

A. Unitarization of Dipole Scattering

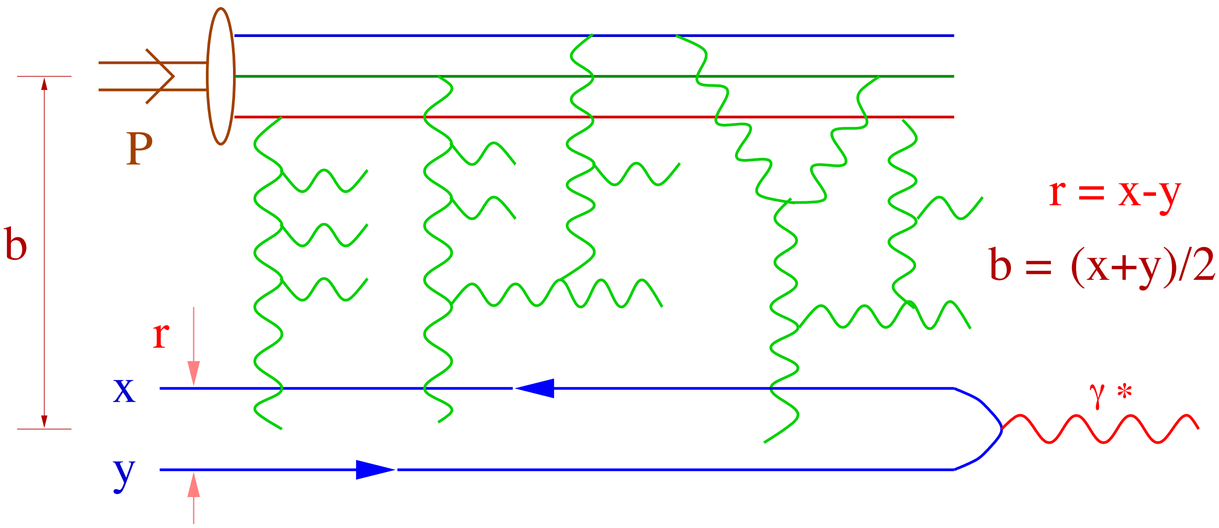

- Recall: Dipole factorization

$$\sigma_{\gamma^* p}(x, Q^2) \;=\; \int_0^1 dz \int d^2\boldsymbol{r}\, \left|\Psi(z,\boldsymbol{r};Q^2)\right|^2 \sigma_{\rm dipole}(x,\boldsymbol{r})$$

$$\sigma_{\rm dipole}(x,\boldsymbol{r}) = 2\int \mathrm{d}^2\boldsymbol{b}\Big(1 - S(x,\boldsymbol{r},\boldsymbol{b})\Big) \equiv 2\int \mathrm{d}^2\boldsymbol{b}\,\mathcal{N}_Y(\boldsymbol{r},\boldsymbol{b})$$

$$\underbrace{S(x,\boldsymbol{r},\boldsymbol{b})}_{\text{S-matrix}} \;=\; \frac{1}{N_c}\left\langle \mathrm{tr}\, V^\dagger(\boldsymbol{x})\, V(\boldsymbol{y})\right\rangle_Y \;\equiv\; 1 - \underbrace{\mathcal{N}_Y(\boldsymbol{r},\boldsymbol{b})}_{\text{scatt. amplitude}}$$

$$V^\dagger(\boldsymbol{x}) \;\equiv \mathrm{P}\ \exp\left\{ ig\int \mathrm{d}x^-\alpha_a(x^-,\boldsymbol{x})T^a\right\}$$

- Weak field (low density) regime: $V^\dagger(\boldsymbol{x}) \approx 1 + ig\alpha(\boldsymbol{x})$

$$\mathcal{N}_Y(\boldsymbol{r}) \sim \alpha_s \boldsymbol{r}^2 \, \frac{xG(x, 1/\boldsymbol{r}^2)}{\pi R^2}$$

$\Longrightarrow$ for x low enough and/or r large enough:

Violation of the unitarity bound $\mathcal{N}_Y(\boldsymbol{r}) \leq 1$!

- However, when $r \gtrsim 1/Q_s(Y)$, the dipole is probing strong fields ($g\alpha \sim 1$), for which :

$$\langle V^\dagger(\boldsymbol{x}) V(\boldsymbol{y}) \rangle_Y \ll 1 \quad \text{for} \quad |\boldsymbol{x} - \boldsymbol{y}| \gg 1/Q_s(Y)$$

$\boxed{1/Q_s(Y) : \text{correlation length for the Wilson lines}}$

- Dipole Unitarization: $\mathcal{N}_Y(\boldsymbol{r}) \sim 1$ for $r \gtrsim 1/Q_s(Y)$

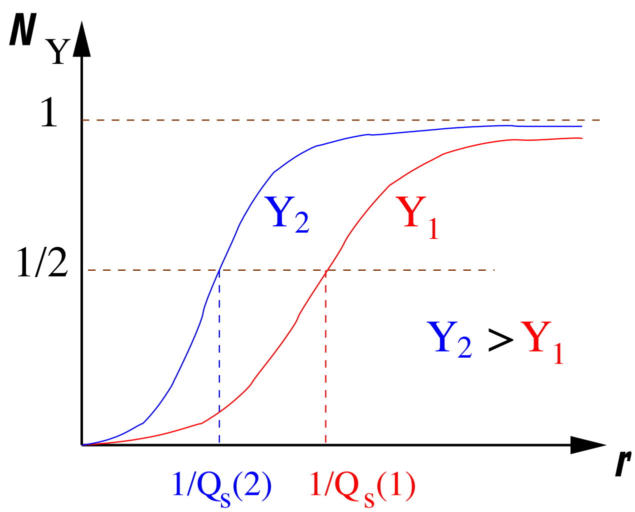

- For an inhomogeneous target, this holds at fixed impact parameter:

$\mathcal{N}_Y(\boldsymbol{r}, \boldsymbol{b}) \simeq 1$ ("blackness") for $r \gtrsim 1/Q_s(Y, \boldsymbol{b})$

B. The Balitsky–Kovchegov equation

- An evolution equation for $S_Y(\boldsymbol{x},\boldsymbol{y})$:

$$\frac{\partial}{\partial Y}\left\langle \mathrm{tr}(V_{\boldsymbol{x}}^{\dagger}V_{\boldsymbol{y}})\right\rangle_Y = \alpha_s \int_{\boldsymbol{z}} \frac{(\boldsymbol{x}-\boldsymbol{y})^2}{(\boldsymbol{x}-\boldsymbol{z})^2(\boldsymbol{y}-\boldsymbol{z})^2} \Big\langle -N_c\,\underbrace{\mathrm{tr}(V_{\boldsymbol{x}}^{\dagger}V_{\boldsymbol{y}})}_{\text{2-point ftion}} + \underbrace{\mathrm{tr}(V_{\boldsymbol{x}}^{\dagger}V_{\boldsymbol{z}})\,\mathrm{tr}(V_{\boldsymbol{z}}^{\dagger}V_{\boldsymbol{y}})}_{\text{4-point ftion}}\Big\rangle_Y$$

- Balitsky (96): First equation in an infinite hierarchy!

- A <u>closed</u> equation can be obtained assuming only 2-point correlations + Large $N_c \gg 1$:

$$\left\langle \mathrm{tr}(V_{\boldsymbol{x}}^{\dagger}V_{\boldsymbol{z}})\,\mathrm{tr}(V_{\boldsymbol{z}}^{\dagger}V_{\boldsymbol{y}})\right\rangle_Y \approx \left\langle \mathrm{tr}(V_{\boldsymbol{x}}^{\dagger}V_{\boldsymbol{z}})\right\rangle_Y \left\langle \mathrm{tr}(V_{\boldsymbol{z}}^{\dagger}V_{\boldsymbol{y}})\right\rangle_Y$$

$\Longrightarrow$ Kovchegov's equation (99):

$$\frac{\partial}{\partial Y} S_Y(\boldsymbol{x},\boldsymbol{y}) \;=\; \bar{\alpha}_s \int_{\boldsymbol{z}} \frac{(\boldsymbol{x}-\boldsymbol{y})^2}{(\boldsymbol{x}-\boldsymbol{z})^2(\boldsymbol{y}-\boldsymbol{z})^2} \Big\{ - S_Y(\boldsymbol{x},\boldsymbol{y}) + S_Y(\boldsymbol{x},\boldsymbol{z}) S_Y(\boldsymbol{z},\boldsymbol{y})\Big\}$$

Strictly justified, e.g., for a large nucleus ($A \gg 1$).
Simple toy equation to study unitarization !

- Alternatively, an equation for $\mathcal{N}_Y = 1 - \mathcal{S}_Y$:

$$\frac{\partial}{\partial Y} \mathcal{N}_Y(\boldsymbol{x},\boldsymbol{y}) \;=\; \bar{\alpha}_s \int_{\boldsymbol{z}} \frac{(\boldsymbol{x}-\boldsymbol{y})^2}{(\boldsymbol{x}-\boldsymbol{z})^2(\boldsymbol{y}-\boldsymbol{z})^2} \Big\{ \underbrace{-\mathcal{N}_Y(\boldsymbol{x},\boldsymbol{y}) + \mathcal{N}_Y(\boldsymbol{x},\boldsymbol{z}) + \mathcal{N}_Y(\boldsymbol{z},\boldsymbol{y})}_{\text{BFKL}} \underbrace{- \mathcal{N}_Y(\boldsymbol{x},\boldsymbol{z})\mathcal{N}_Y(\boldsymbol{z},\boldsymbol{y})}_{\text{Non-linear}} \Big\} \, .$$

- Very complete numerical studies, which exhibit :

  — unitarization ($\mathcal{N}_Y \simeq 1$) for $r \gtrsim 1/Q_s(Y)$

  — the energy dependence of $Q_s(Y)$

  [Armesto, Braun, 01; Golec-Biernat, Motyka, Stasto, 01]

  — suppression of infrared diffusion

  [Golec-Biernat, Motyka, Stasto, 01]

  — geometric scaling at saturation ($r \gtrsim 1/Q_s$)

  — geometric scaling <u>below</u> saturation ($r < 1/Q_s$), down to rather small values of $rQ_s(Y)$.

  [Levin, Tuchin, 01; Golec-Biernat, Motyka, Stasto, 01; Lublinsky, 02]

  — impact parameter dependence and violation of Froissart bound [Golec-Biernat, Stasto, 03]

  — applications to the phenomenology of DIS at HERA [Gotsman, Levin, Lublinsky, Maor (02)]

  and of heavy ion collisions at RHIC (“Cronin effect”)

  [Albacete, Armesto, Kovner, Salgado, Wiedemann, 03]

- All these features have been confirmed and further studied by Rummukainen, Weigert (03), via a <u>direct resolution of the functional RGE on a lattice.</u>

- Approximate analytic solutions:

  Physical content is even more manifest !

  Kovchegov, 99; Levin, Tuchin, 00–01; E.I., McLerran, 2001; E.I., Itakura, McLerran, 2002; Mueller, Triantafyllopoulos, 02; E.I., Mueller 03; Munier, Peschanski, 03

- Small dipole ($r \ll 1/Q_s(Y)$) $\Longrightarrow$ BFKL eq.

$$\mathcal{N}_Y(\boldsymbol{r}) \approx \left(\boldsymbol{r}^2 Q_0^2\right)^{1/2} \mathrm{e}^{\omega \bar{\alpha}_s Y} \exp\left\{-\frac{\ln^2\left(1/\boldsymbol{r}^2 Q_0^2\right)}{2\beta\bar{\alpha}_s Y}\right\}$$

- Saturation condition:

  $\mathcal{N}_Y(\boldsymbol{r}) \sim \mathcal{N}_0$ when $r \sim 1/Q_s(Y)$ (say, $\mathcal{N}_0 = 0.5$)

$$\boxed{Q_s^2(Y) \simeq Q_0^2\,\mathrm{e}^{\lambda Y} \text{ with } \lambda \simeq 4.8\bar{\alpha}_s}$$

- Replace Q_0 by $Q_s(Y)$ as the reference scale:

$$\mathcal{N}_Y(\boldsymbol{r}) \approx \mathcal{N}_0\left(\boldsymbol{r}^2 Q_0^2\right)^{\gamma_s} \exp\left\{-\frac{\ln^2\left(1/\boldsymbol{r}^2 Q_s^2(Y)\right)}{2\beta\bar{\alpha}_s Y}\right\}$$

- For r near $1/Q_s(Y) \Longrightarrow$ Geometric scaling :

$$\boxed{\mathcal{N}_Y(\boldsymbol{r}) \approx \mathcal{N}_0\left(\boldsymbol{r}^2 Q_0^2\right)^{\gamma_s} \text{ with } \gamma_s \simeq 0.63}$$

- Large dipole: $r \gg 1/Q_s(Y) \Longrightarrow$ Simple eq. for $S_Y(\boldsymbol{r})$

$$\mathcal{N}_Y(\boldsymbol{r}) \approx 1 - \kappa \exp\left\{-\frac{1}{4c}\ln^2\left(\boldsymbol{r}^2 Q_s^2(Y)\right)\right\}$$

  with $c \simeq 4.8$ [Levin, Tuchin, 00; E.I., Mueller 03]

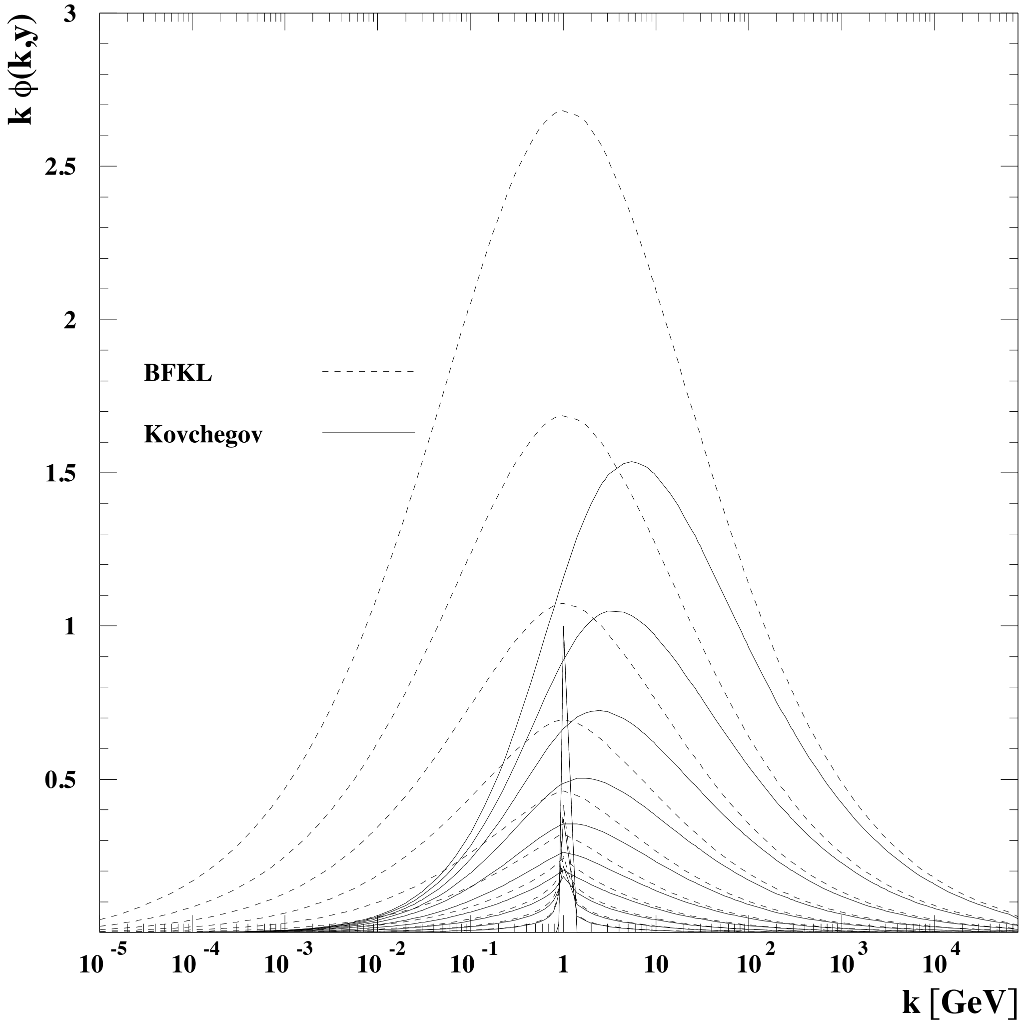

Figure 1: The functions $k\phi(k,Y)$ constructed from solutions to the BFKL and the Balitsky-Kovchegov equations for different values of the evolution parameter $Y = \ln(1/x)$ ranging from 1 to 10. The coupling constant $\alpha_s = 0.2$.

From K. Golec-Biernat, L. Motyka, A. M. Stasto, Phys Rev D65 (2002) 074037; hep-ph/0110325

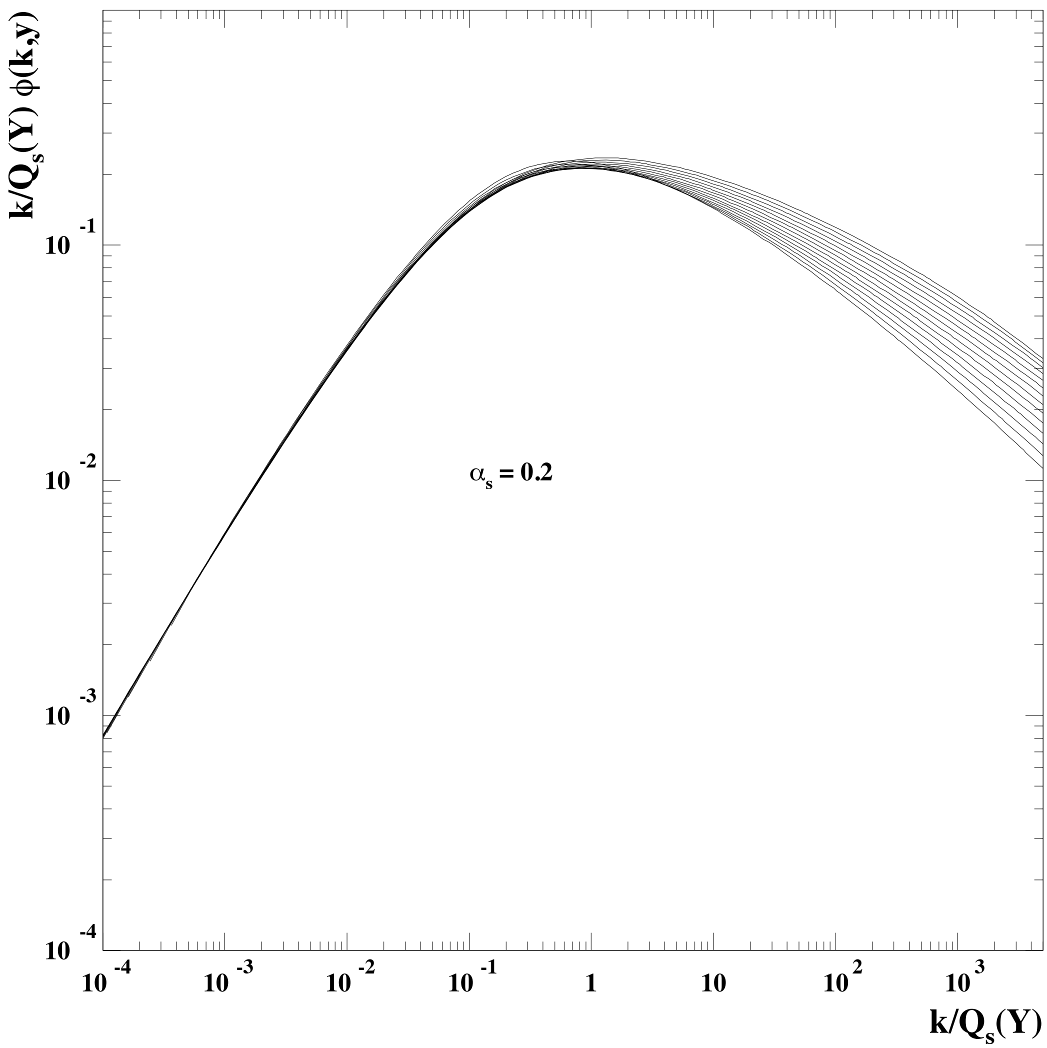

Figure 2: The function $(k/Q_s(Y))\,\phi(k,Y)$ plotted versus $k/Q_s(Y)$ for different values of rapidity Y ranging from 10 to 23. The saturation scale $Q_s(Y)$ corresponds to the position of the maximum of the function $k\,\phi(k,Y)$.

From K. Golec-Biernat, L. Motyka, A. M. Stasto, Phys Rev D65 (2002) 074037; hep-ph/0110325

C. Saturation & Geometric Scaling at HERA

1. The Golec-Biernat–Wüsthoff model (1999)

$$\sigma_{\rm dipole}(x, \boldsymbol{r}) \;=\; \sigma_0 \left(1 - \exp\left\{ - \frac{\boldsymbol{r}^2 Q_s^2(x)}{4} \right\}\right)$$

$$Q_s^2(x) = 1{\rm GeV}^2\, (x_0/x)^{\lambda}$$

- "Saturation" : unitarization ($\sigma_{\rm dipole}(x, r_\perp) \simeq \sigma_0$) over a energy dependent scale $1/Q_s(x)$

- High $Q^2 \gg Q_s^2(x)$:

  $F_2(x, Q^2) \;\sim\; \sigma_0\, Q_s^2(x)\, \ln\big(Q^2/Q_s^2(x)\big) \;\propto x^{-\lambda}$

  $Q_s(x)$ acts effectively as an infrared cutoff

- Low $Q^2 \ll Q_s^2(x)$:

  $F_2(x, Q^2) \sim \sigma_0\, Q^2 \ln\big(Q_s^2(x)/Q^2\big) \;\; \propto \ln(1/x)$

- Remarkably good fit to the (old) small–x data at HERA (F_2, F_2^D) at $x < 0.01$ with only 3 parameters

  $\sigma_0 = 23\,{\rm mb}, \quad x_0 = 3\times 10^{-4}, \quad \lambda \simeq 0.3$

- 'Hard' saturation scale: $Q_s \geq 1$ GeV for $x \leq 10^{-4}$

- Good description of the 'hard–to–soft' transition in F_2 with lowering Q^2

- No QCD evolution at small $r_\perp$:

  $\sigma_{\rm dipole}(x, \boldsymbol{r}) \;\propto\; \boldsymbol{r}^2 Q_s^2(x)$ instead of $\boldsymbol{r}^2 xG(x, 1/\boldsymbol{r}^2)$

- No impact parameter dependence

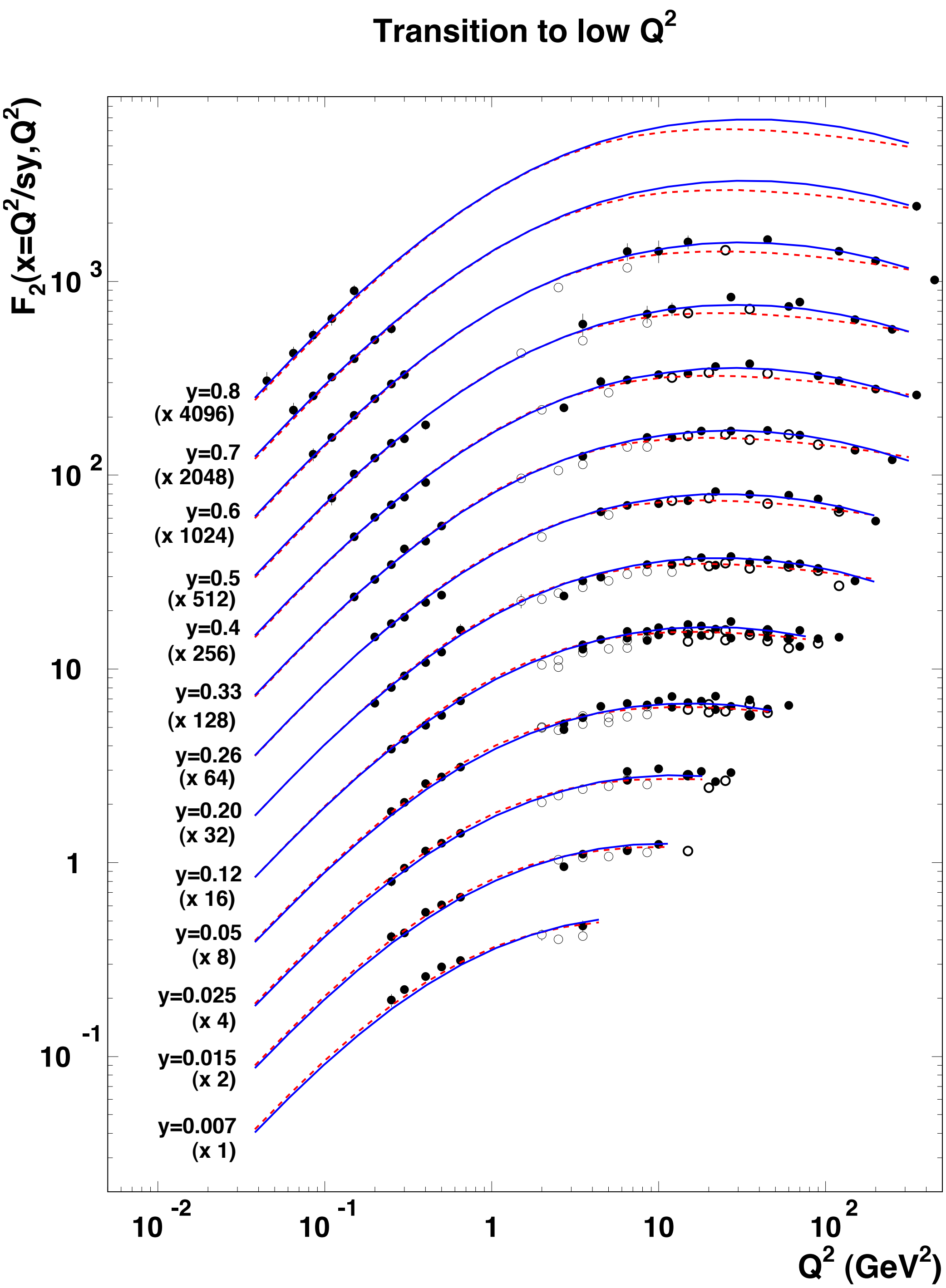

Figure 3: $F_2(x,Q^2)$ *as a function of* Q^2 *for fixed* $y = Q^2/(sx)$*. The solid lines: the model with DGLAP evolution by BGBK and the dashed lines: the saturation model by GBW. The curves are plotted for* $x < 0.01$*. Full circles: ZEUS data and open circles: H1 data.*

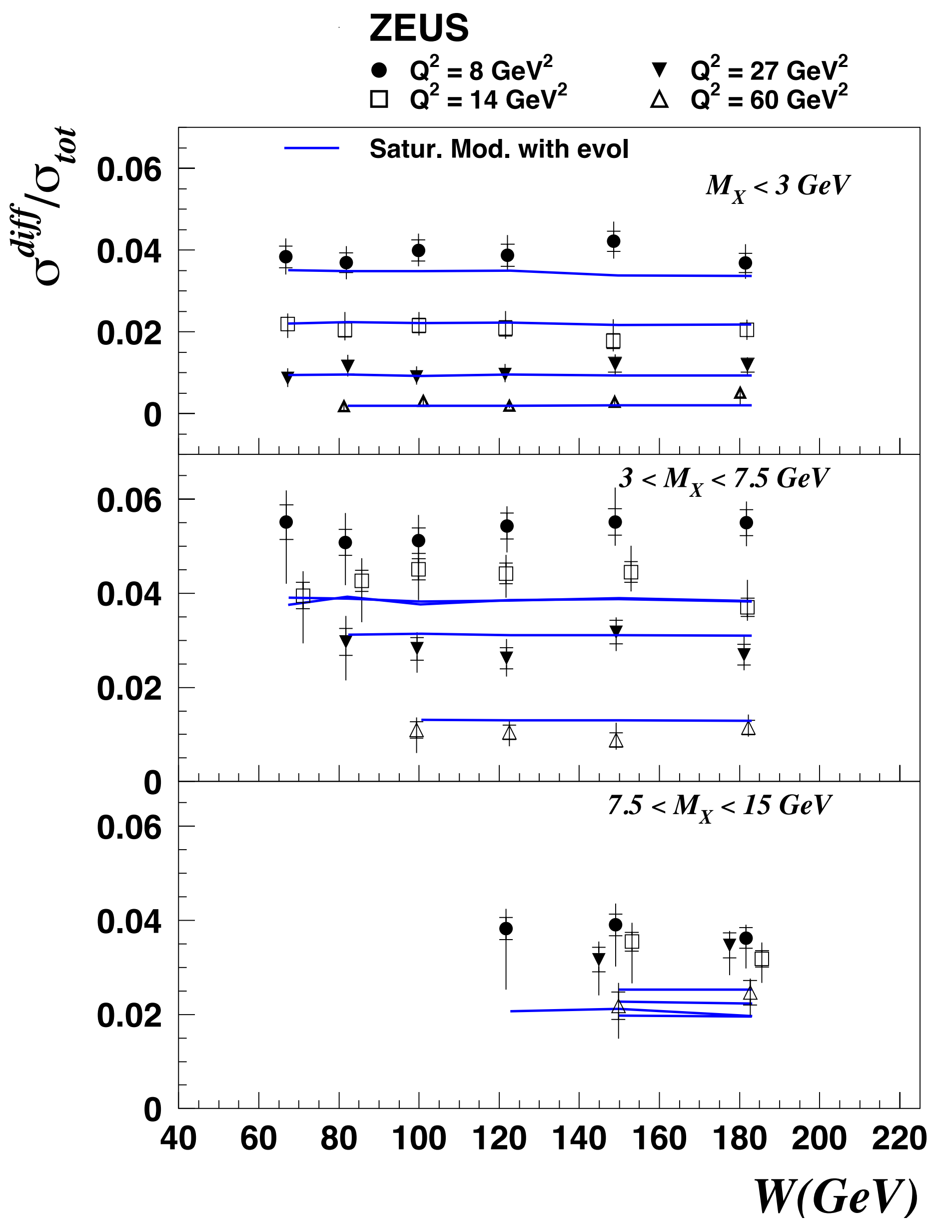

Figure 4: The ratio of $\sigma_{diff}/\sigma_{tot}$ versus the $\gamma^* p$ energy W. The data is from ZEUS and the solid lines correspond to the results of the DGLAP improved model with massless quarks (BGBK).

2. Geometric Scaling at HERA

- GBW model: $\sigma_{\text{dipole}}(x, \boldsymbol{r}) \equiv \sigma\big(\boldsymbol{r}^2 Q_s^2(x)\big)$

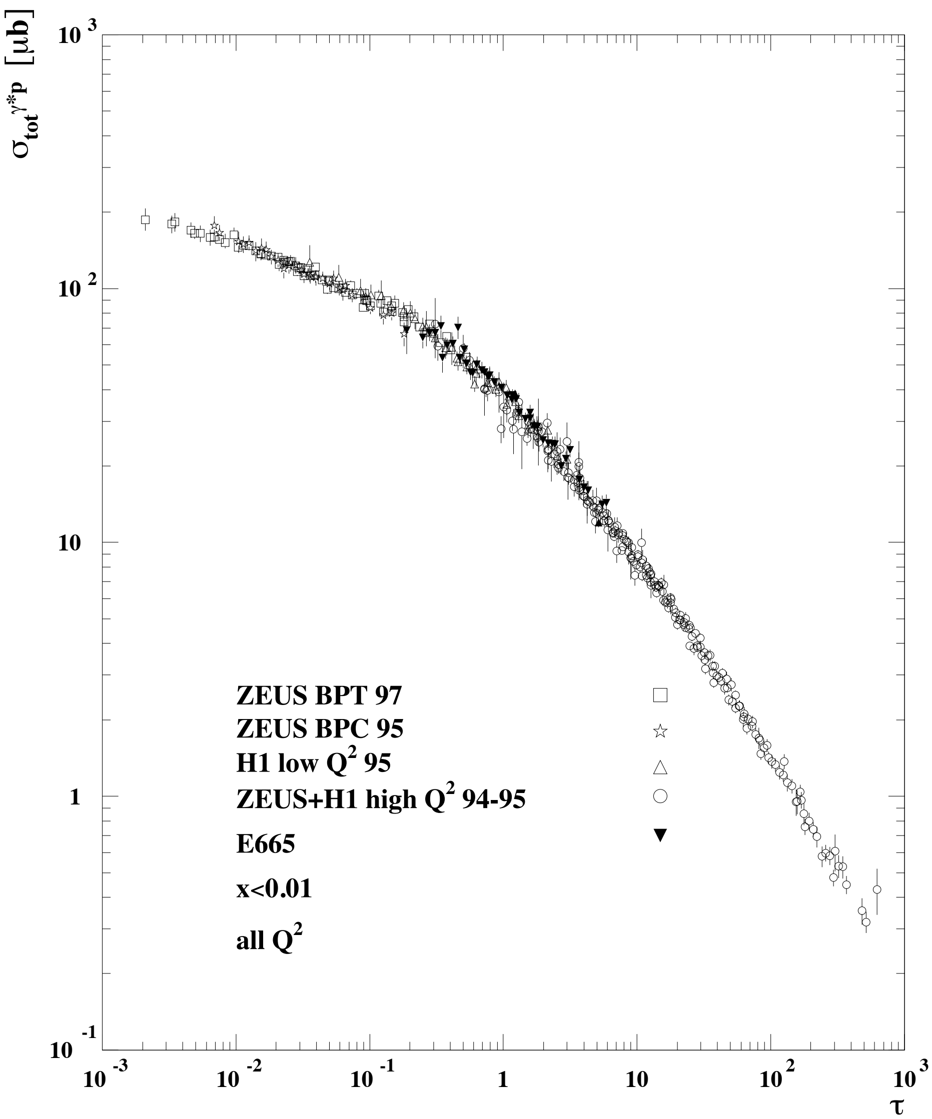

- Staśto, Golec-Biernat, and Kwieciński, 2000 :

  For $x < 10^{-2}$ and $Q^2 \lesssim 400\text{GeV}^2$, data show (approximate) scaling:

$$\sigma_{\gamma^* p}(x, Q^2) \approx \sigma(\tau), \qquad \text{with } \tau \equiv \frac{Q^2}{Q_s^2(x)}$$

3. A CGC fit to the HERA data

- Improving the GBW model:

  — DGLAP improvement by Bartels, Golec-Biernat, Kowalski (02)

  $$\sigma_{\rm dipole}(x,\boldsymbol{r}) \,=\, \sigma_0\Big(1-\exp\{-\alpha_s \boldsymbol{r}^2 xG(x,1/\boldsymbol{r}^2)\}\Big)$$

  (Glauber-like exponentiation)

  — Adding the b–depedence: Kowalski, Teaney (03)

  $$xG(x,1/\boldsymbol{r}^2)T(b) \quad \text{with} \quad T(B) = \frac{1}{2\pi R^2}\exp\left(-b^2/2R\right)$$

  — Adding BK dynamics by Gotsman, Levin, Lublinsky, Maor (03)

  Numerical matching of BK and DGLAP

  $\Longrightarrow$ Rather good global fits !

- Can we directly probe the BFKL dynamics towards saturation ?

  — Anomalous dimension < 1

  — Geometric scaling near Q_s

  — Scaling violations by the diffusion term

  — Saturation exponent $\lambda \simeq 0.3$

- Focus on smallish Q^2 : up to 50 GeV^2

- Use analytic results for the dipole amplitude

- The CGC fit (E.I., Itakura, Munier, 03)

  $\sigma_{\rm dipole}(x,\boldsymbol{r}) = 2\pi R^2 \mathcal{N}(rQ_s, Y)$

$$\mathcal{N}(rQ_s,Y) \;=\; \mathcal{N}_0 \left(\frac{r^2 Q_s^2}{4}\right)^{\gamma + \frac{\ln(2/rQ_s)}{\kappa\lambda Y}} \qquad \text{for} \quad rQ_s \le 2,$$

$$\mathcal{N}(rQ_s,Y) \;=\; 1 - \mathrm{e}^{-a\ln^2(b\,rQ_s)} \qquad \text{for} \quad rQ_s > 2,$$

  $Q_s \equiv Q_s(x) = (x_0/x)^{\lambda/2}$ GeV

  $\gamma = 0.63, \quad \kappa = 9.9$ (fixed by BFKL)

  a, b : fixed by continuity at $rQ_s = 2$

  $\Longrightarrow$ The same 3 parameters as in the GBW model:

  R, x_0 and λ

- BFKL anomalous dimension at saturation : $\gamma = 0.63$

- Effective anomalous dimension :

$$\gamma_{\rm eff}(rQ_s,Y) \equiv -\frac{d\ln\mathcal{N}(rQ_s,Y)}{d\ln(4/r^2Q_s^2)} = \gamma_s + 2\,\frac{\ln(2/rQ_s)}{\kappa\lambda Y}$$

  $\Longrightarrow$ Scaling violation !

- Fit to the ZEUS data for $F_2(x,Q^2)$ within the range:

$$\boxed{x \le 10^{-2} \text{ and } 0.045 \le Q^2 \le 45\,\mathrm{GeV}^2}$$

  (156 data points)

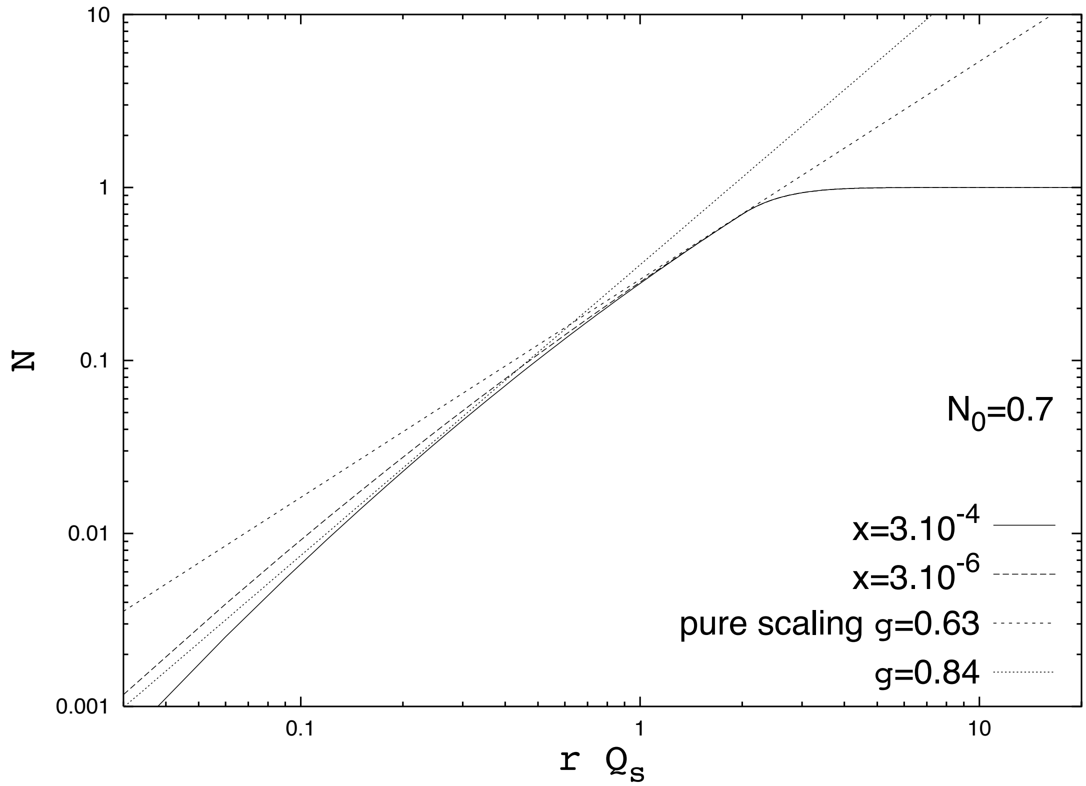

Figure 5: The dipole amplitude for two values of x, compared to the pure scaling functions with "anomalous dimension" $\gamma = \gamma_s = 0.63$ and $\gamma = 0.84$.

$$\gamma_{\text{eff}}(rQ_s, Y) \equiv -\frac{d\ln\mathcal{N}(rQ_s, Y)}{d\ln(4/r^2Q_s^2)} = \gamma_s + 2\,\frac{\ln(2/rQ_s)}{\kappa\lambda Y}$$

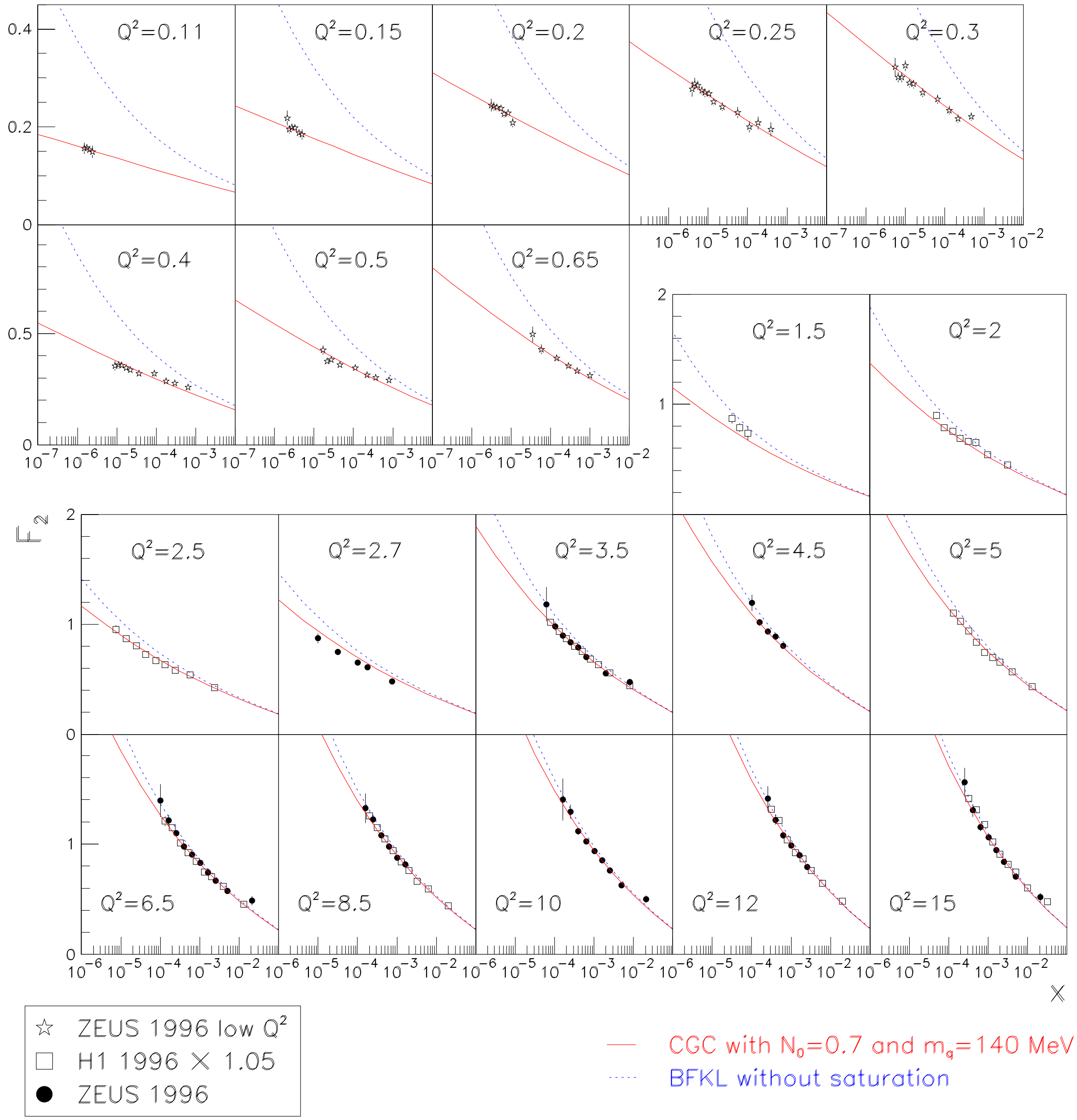

Figure 6: The F_2 structure function in bins of Q^2 for small (upper part) and moderate (lower part) values of Q^2. The full line shows the result of the CGC fit with $\mathcal{N}_0 = 0.7$ to the ZEUS data for $x \leq 10^{-2}$ and $Q^2 \leq 45$ GeV^2. The dashed line shows the predictions of the pure BFKL part of the fit (no saturation).

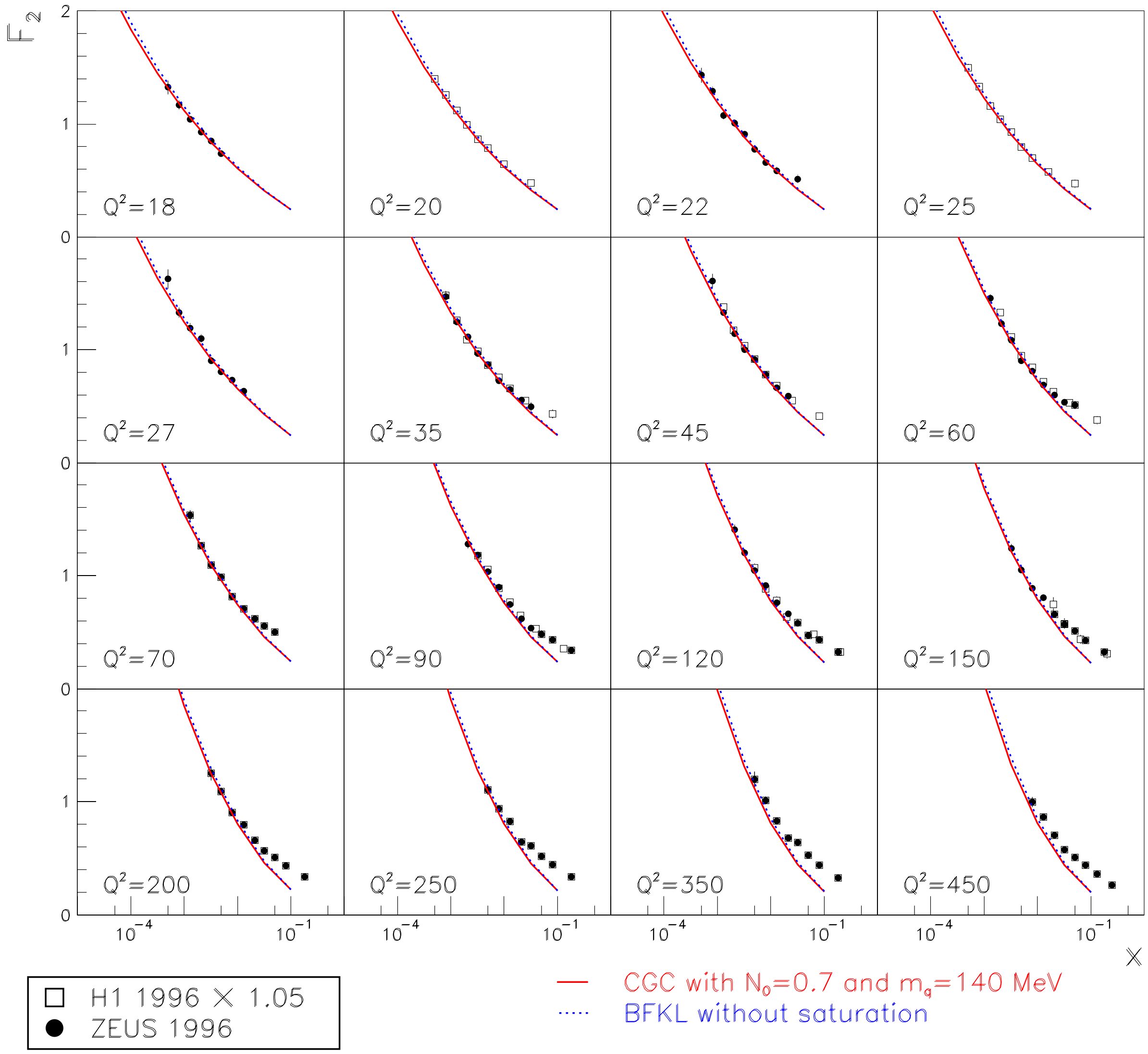

Figure 7: The same as before, but for large Q^2. Note that in the bins with $Q^2 \geq 60\,\mathrm{GeV}^2$, the CGC fit is extrapolated outside the range of the fit ($Q^2 < 50$ GeV^2 and $x \leq 10^{-2}$), to better emphasize its limitations.

$\mathcal{N}_0$/model	0.5	0.6	0.7	0.8	0.9	GBW
χ^2	146.43	129.88	123.63	125.61	133.73	243.87
χ^2/d.o.f	0.96	0.85	0.81	0.82	0.87	1.59
x_0 ($\times 10^{-4}$)	0.669	0.435	0.267	0.171	0.108	4.45
λ	0.252	0.254	0.253	0.252	0.250	0.286
R (fm)	0.692	0.660	0.641	0.627	0.618	0.585

Table 1: The CGC fits for different values of $\mathcal{N}_0$ and 3 quark flavors with mass $m_q = 140$ MeV. Also shown is the fit obtained by using the GBW model.

	$m_q = 50$ MeV			$m_q = 10$ MeV		
$\mathcal{N}_0$	0.5	0.7	0.9	0.5	0.7	0.9
χ^2	148.02	108.52	108.76	149.27	107.64	106.49
χ^2/d.o.f	0.97	0.71	0.71	0.98	0.70	0.70
x_0 ($\times 10^{-4}$)	2.77	0.898	0.333	3.32	1.06	0.382
λ	0.290	0.281	0.274	0.295	0.285	0.276
R (fm)	0.604	0.574	0.561	0.593	0.566	0.554

Table 2: The CGC fits for three values of $\mathcal{N}_0$ and quark masses $m_q = 50$ MeV (left) and $m_q = 10$ MeV (right).

1) $0.25 < \lambda < 0.29$ is in agreement with the NLO BFKL calculation by Triantafyllopoulos (02)

2) Scaling violation is essential to describe the data.

3) Remarkable agreement even at $Q^2 \ll 1$ GeV^2 (quark–hadron duality)

VI. Saturation Physics at RHIC

Geometric Scaling and High-$p_\perp$ Suppression

Kharzeev, Levin, McLerran (02)

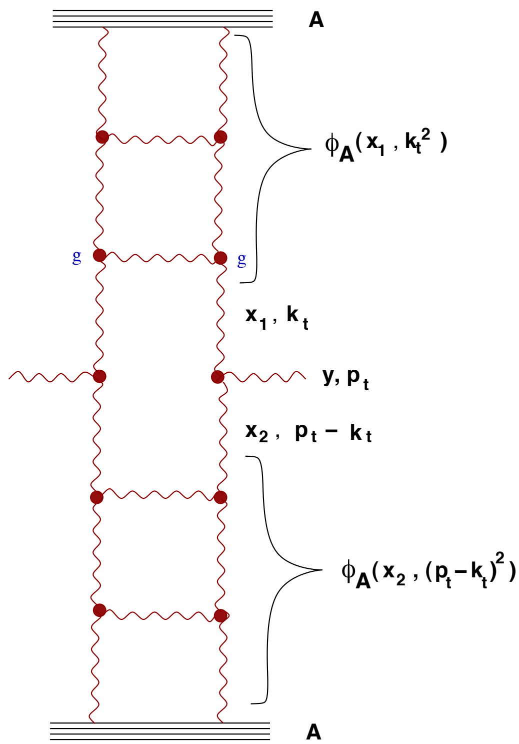

$$\frac{dN}{dyd^2p_\perp} = \frac{\alpha_s}{\pi R_A^2}\frac{1}{p_\perp^2}\int dk_\perp^2\ \alpha_s\ \varphi_A(x_1, k_\perp^2)\ \varphi_A(x_2, (p-k)_\perp^2)$$

- $\varphi_A(x, k_\perp^2)$ = the unintegrated gluon distribution
- $x_{1,2} = (p_\perp/\sqrt{s})\exp(\pm\eta)$
- η = the (pseudo)rapidity of the produced gluon
- $\pi R_A^2 \propto N_{part}^{2/3}$ = the nuclear overlap area
- $Q_s^2(x, A) \propto N_{part}^{1/3}$ = the saturation momentum
  for the considered centrality

- High $p_\perp \gg Q_s^2(x)/\Lambda$: $\varphi_A(x,k_\perp^2) \approx \frac{\pi R_A^2}{\alpha_s}\frac{Q_s^2}{k_\perp^2}$

$$\frac{dN}{dyd^2p_\perp} \sim \frac{\pi R_A^2}{\alpha_s\, p_\perp^2}\int^{p_\perp^2} dk_\perp^2\, \frac{Q_s^2}{k_\perp^2}\,\frac{Q_s^2}{p_\perp^2} \sim \frac{\pi R_A^2 Q_s^4}{\alpha_s\, p_\perp^4} \sim N_{\rm coll}$$

- $Q_s(x) < p_\perp < Q_s^2(x)/\Lambda$: $\varphi_A(x,k_\perp^2) \approx \frac{\pi R_A^2}{\alpha_s}(Q_s^2/k_\perp^2)^{1/2}$

$$\frac{\pi R_A^2}{\alpha_s p_\perp^2}\int^{p_\perp^2} dk_\perp^2\, \left(\frac{Q_s^2}{k_\perp^2}\right)^{1/2}\left(\frac{Q_s^2}{p_\perp^2}\right)^{1/2} \sim \frac{\pi R_A^2 Q_s^2}{\alpha_s p_\perp^2} \sim N_{\rm part}$$

- Low $p_\perp < Q_s(x)$: $\varphi_A(x,k_\perp^2) \approx \frac{\pi R_A^2}{\alpha_s}$

$$\frac{dN}{dyd^2p_\perp} \sim \frac{\pi R_A^2}{\alpha_s\, p_\perp^2}\int^{Q_s^2} dk_\perp^2 \sim \frac{\pi R_A^2 Q_s^2}{\alpha_s\, p_\perp^2} \sim N_{\rm part}$$

- “Nuclear modification factor”:

The ratio of the AA to the $p+p$ hadron yields scaled by nuclear geometry (T_{AB}) :

$$R_{AA}(p_T) = \frac{d^2N^{\pi^0}_{AA}/dydp_T}{\langle T_{AB}\rangle \times d^2\sigma^{\pi^0}_{pp}/dydp_T}$$

$R_{AA}(p_T)$ measures the deviation of AA from an incoherent superposition of NN collisions in terms of suppression (R_{AA} <1) or enhancement (R_{AA} >1).

The RHIC data for Au–Au collision at $s = 130$ GeV^2 and $s = 200$ GeV^2 show a significant suppression (by a factor of 4 to 5), and are consistent within the error bars with $N_{\rm part}$–scaling !

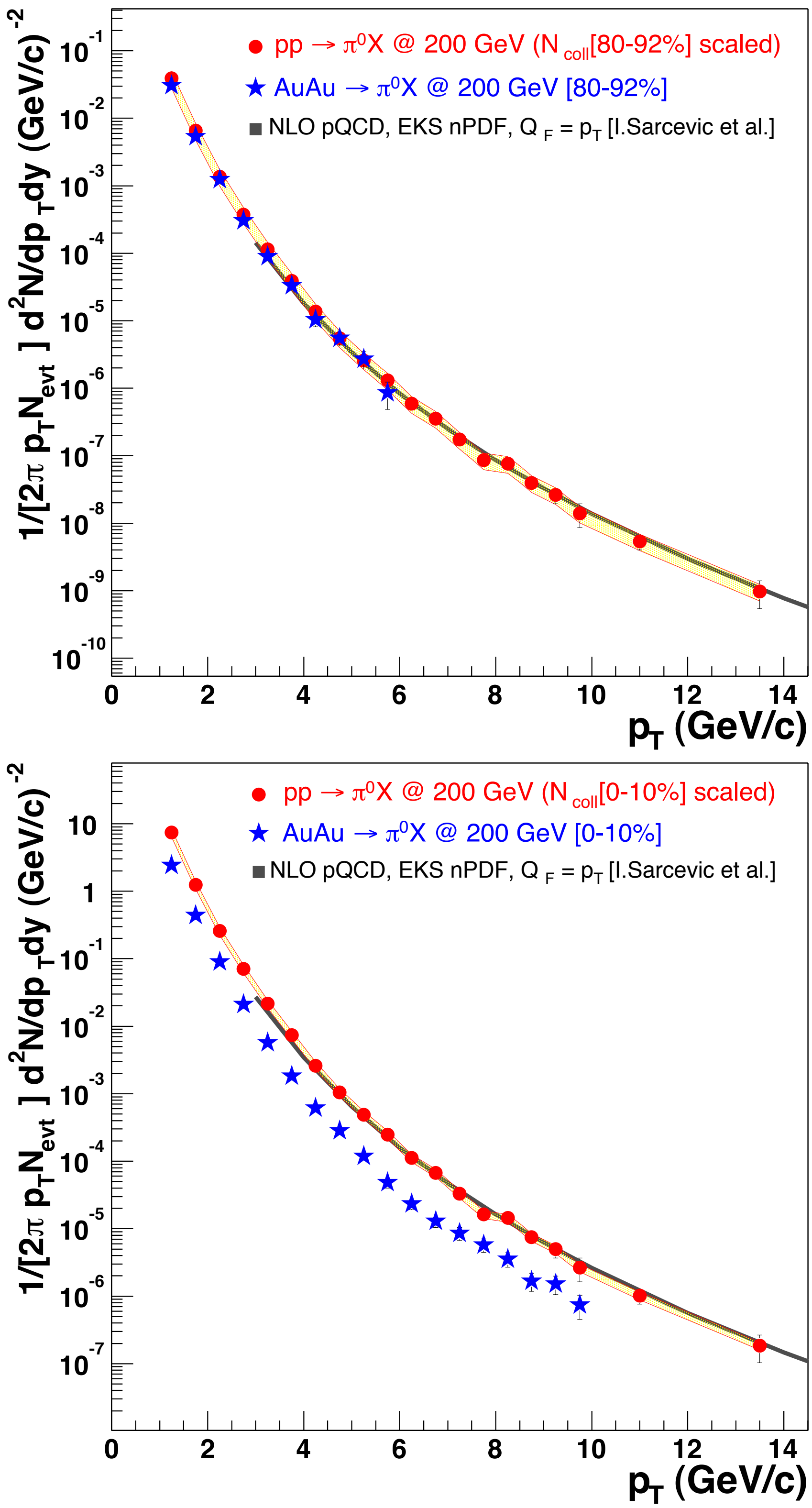

Figure 8: Invariant π^0 yields measured by PHENIX in peripheral (*left*) and in central (*right*) Au+Au collisions (stars), compared to the N_{coll} scaled p+p π^0 yields (circles) and to a NLO pQCD calculation (gray line). The yellow band around the scaled p+p points includes in quadrature the absolute normalization errors in the p+p and Au+Au spectra as well as the uncertainties in T_{AB}. From the recent review by D. d'Enterria, nucl-ex/0309015.

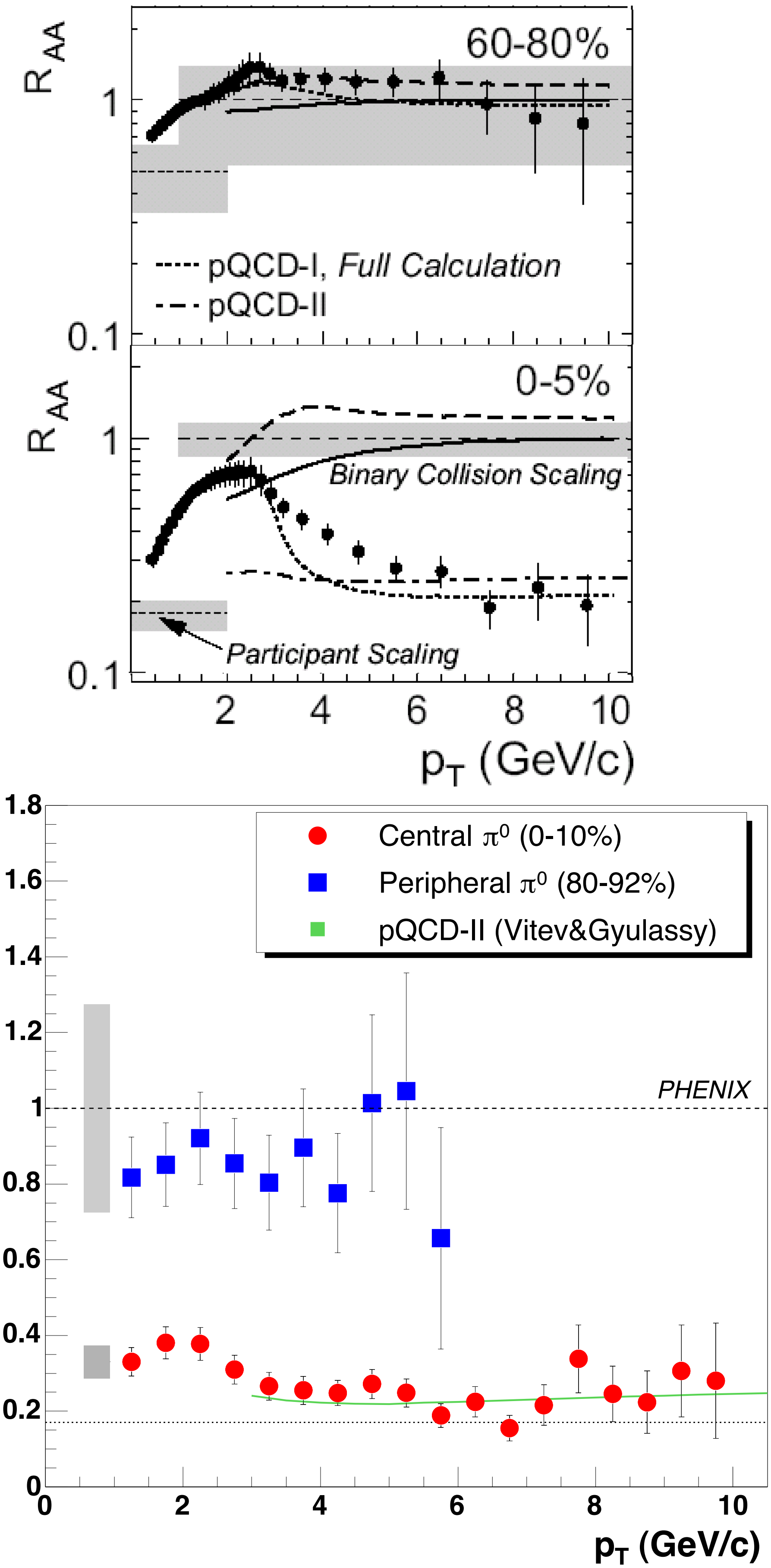

Figure 9: Nuclear modification factor, $R_{AA}(p_T)$, in peripheral and central Au+Au reactions for charged hadrons (*left*) and π^0 (*right*) measured at $\sqrt{s_{NN}} = 200$ GeV by STAR and PHENIX respectively. A comparison to theoretical curves:

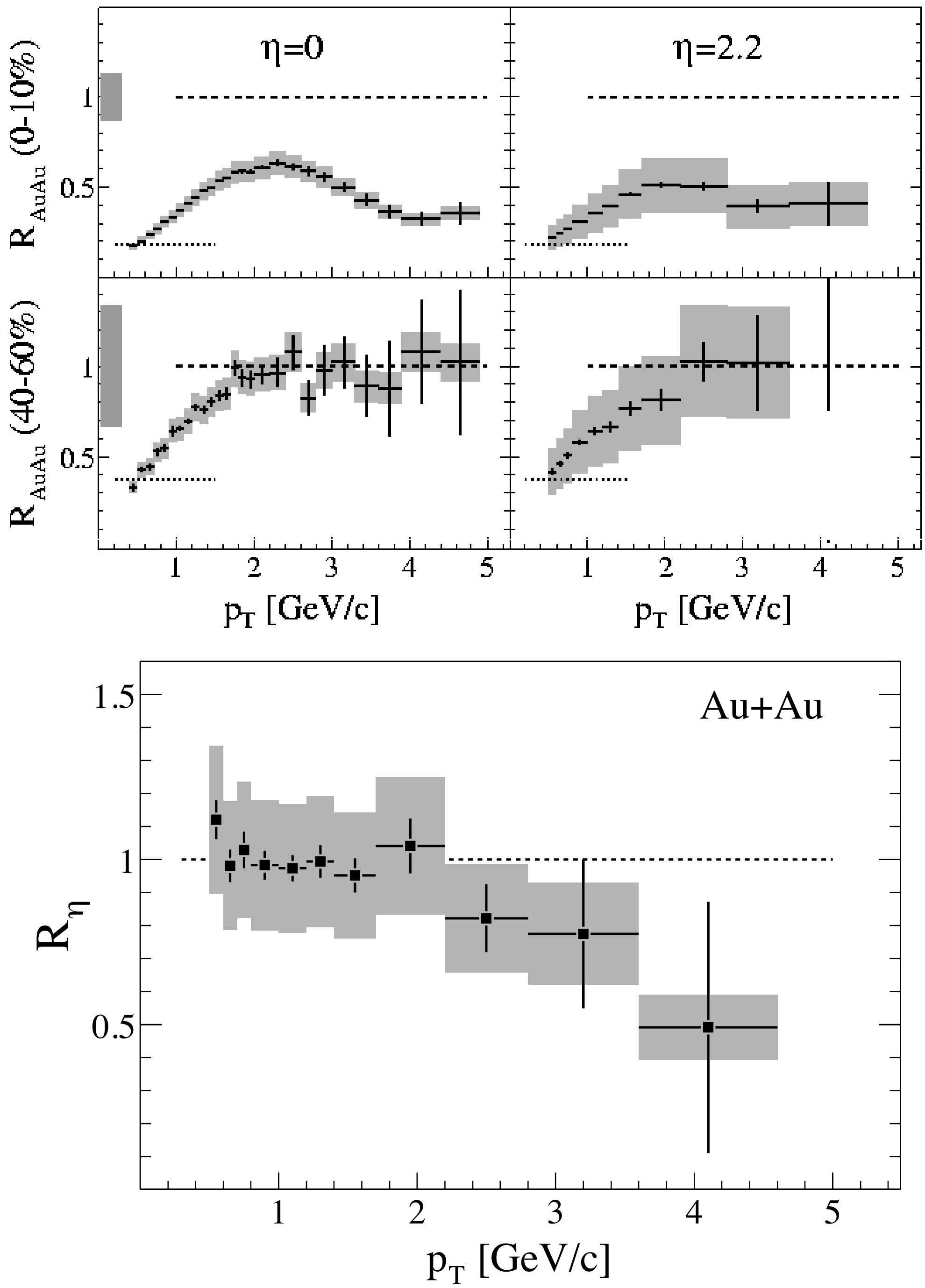

Figure 10: *Left*: $R_{AA}(p_T)$ measured by BRAHMS at $\eta = 0$ and $\eta = 2.2$ for 0–10% most central and for semi-peripheral (40-60%) Au+Au collisions. *Right*: Ratio R_η of R_{cp} distributions at $\eta = 2.2$ and $\eta = 0$. From D. d'Enterria, nucl-ex/0309015